2017 Fall

"Phase Transformation *in* Materials"

11.29.2017

Eun Soo Park

Office: 33-313
Telephone: 880-7221
Email: espark@snu.ac.kr
Office hours: by an appointment

Contents for previous class

< Phase Transformation in Solids >

1) Diffusional Transformation

(a) Precipitation

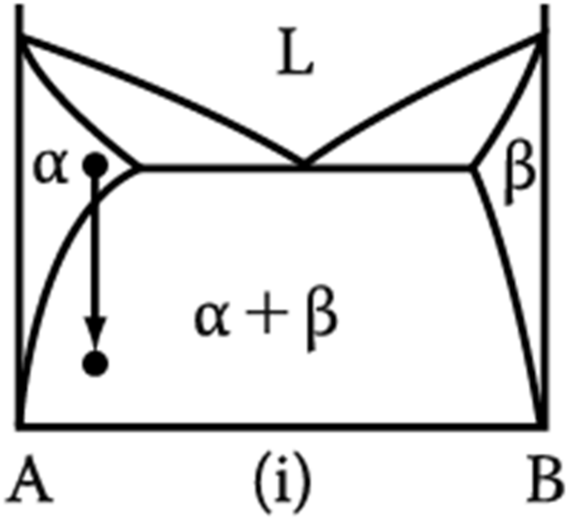

Homogeneous Nucleation

➡ Effect of misfit strain energy

$$\Delta G = \boxed{-V\Delta G_V} + \boxed{A\gamma + V\Delta G_S}$$

$$r^* = \frac{2\gamma}{(\Delta G_V - \Delta G_S)} \quad \Delta G^* = \frac{16\pi\gamma^3}{3(\Delta G_V - \Delta G_S)^2}$$

$$N_{\text{hom}} = \omega C_0 \boxed{\exp\left(-\frac{\Delta G_m}{kT}\right)} \boxed{\exp\left(-\frac{\Delta G^*}{kT}\right)}$$

Heterogeneous Nucleation

➡ suitable nucleation sites ~ nonequilibrium defects

(creation of nucleus~destruction of a defect($-\Delta G_d$))

$$\boxed{\Delta G_{het} = -V(\Delta G_V - \Delta G_S) + A\gamma - \Delta G_d}$$

$$\frac{\Delta G^*_{het}}{\Delta G^*_{\text{hom}}} = \frac{V^*_{het}}{V^*_{\text{hom}}} = S(\theta)$$

$$\boxed{\frac{N_{het}}{N_{\text{hom}}} = \frac{C_1}{C_0} \exp\left(\frac{\Delta G^*_{\text{hom}} - \Delta G^*_{het}}{kT}\right)}$$

Rate of Homogeneous Nucleation Varies with undercooling below T_e for alloy X_0

Effective equilibrium temperature is reduced by **misfit strain E term, ΔGs.**

Thermodynamics

vs

Kinetics

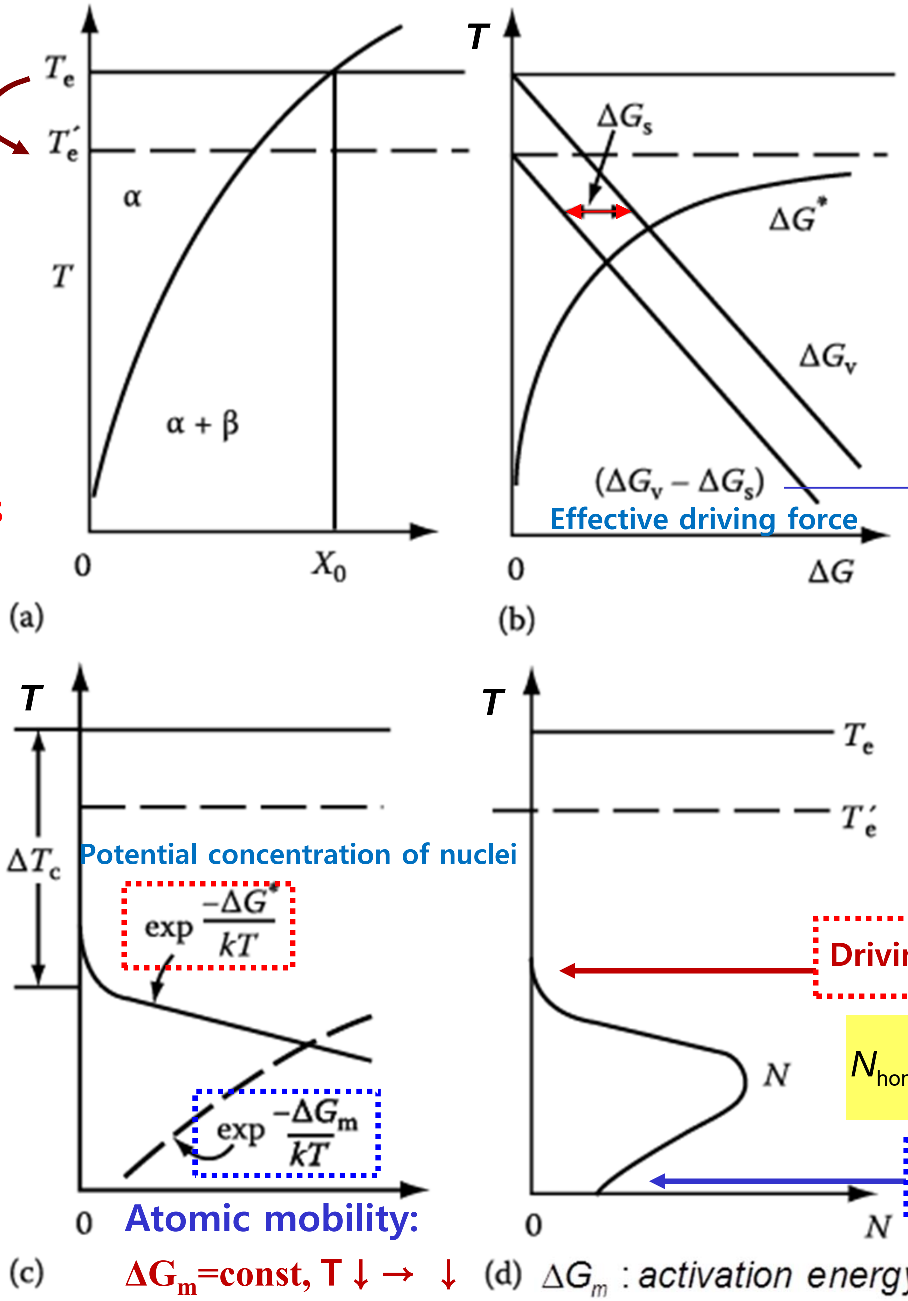

Effective driving force

$$\Delta G_V \propto \Delta X \propto \Delta T$$

Composition dependent

$$\Delta G^* = \frac{16\pi\gamma^3}{3(\Delta G_V - \Delta G_S)^2}$$

Resultant energy barrier for nucleation

Critical undercooling ΔT_c

Potential concentration of nuclei

Driving force ΔG_v~too small → N~negligible

$$N_{hom} = \omega C_0 \exp\left(-\frac{\Delta G_m}{kT}\right) \exp\left(-\frac{\Delta G^*}{kT}\right)$$

Diffusion~too slow → N~negligible

Atomic mobility:

ΔG_m=const, T ↓ → ↓

ΔG_m : *activation energy for atomic migration*

Heterogeneous Nucleation in Solids

The Rate of Heterogeneous Nucleation during Precipitation

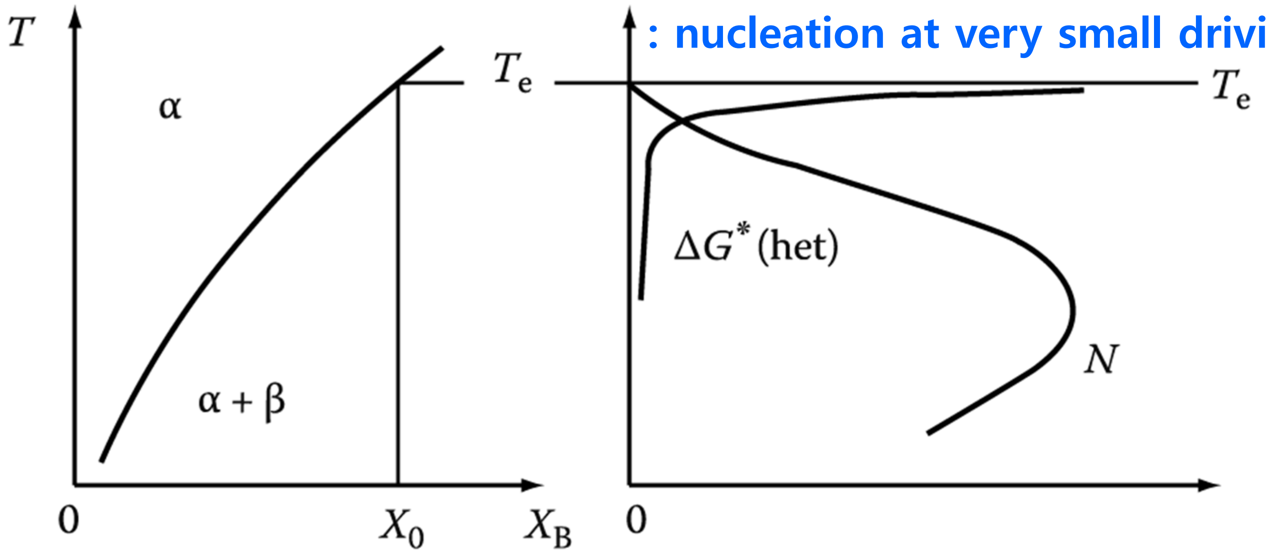

: nucleation at very small driving forces

* Relative magnitudes of the heterogeneous and homogeneous volume nucleation rates

$$\frac{N_{het}}{N_{hom}} = \frac{C_1}{C_0}\exp\left(\frac{\Delta G^*_{hom} - \Delta G^*_{het}}{kT}\right)$$

ω 와 ΔG_m의 차이는 미비하여 무시

ΔG* ~ always smallest for heterogeneous nucleation ⇨ Exponential factor : very large quantity ⇨ $\frac{N_{het}}{N_{hom}} > 1$ High heterogeneous nucleation rate

But, The factor C_1/C_0 ?

Heterogeneous Nucleation in Solids

$$\frac{N_{het}}{N_{hom}} = \frac{C_1}{C_0}\exp\left(\frac{\Delta G^*_{hom} - \Delta G^*_{het}}{kT}\right)$$

C_1/C_0 for Various Heterogeneous Nucleation Sites

각각의 핵생성처에서 경쟁적으로 핵생성 발생: 구동력 조건에 따라 전체 핵생성 속도에 dominant하게 영향을 미치는 site 변화

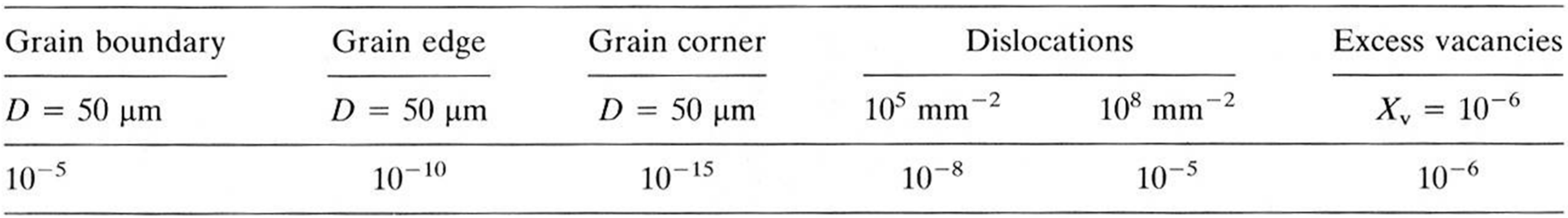

Grain boundary	Grain edge	Grain corner	Dislocations		Excess vacancies
$D = 50\ \mu m$	$D = 50\ \mu m$	$D = 50\ \mu m$	$10^5\ mm^{-2}$	$10^8\ mm^{-2}$	$X_v = 10^{-6}$
10^{-5}	10^{-10}	10^{-15}	10^{-8}	10^{-5}	10^{-6}

In order to make nucleation occur exclusively on the grain corner, how should the alloy be cooled?

1) At very small driving forces (ΔG_v), when activation energy barriers for nucleation are high, the highest nucleation rates will be produced by grain-corner nucleation.

핵생성 구동력

ΔG_v

↓

increase

2) dominant nucleation sites:

grain edges → grain boundaries

3) At very high driving forces it may be possible for the (C_1/C_0) term to dominate and then homogeneous nucleation provides the highest nucleation rates.

* The above comments concerned nucleation during isothermal transformations
(driving force for nucleation: [isothermal] constant ↔ [continuous cooling] increase with time)

- **Precipitate growth**

1) Growth behind Planar Incoherent Interfaces

Diffusion-Controlled Thickening: $x \propto \sqrt{(Dt)}$ Parabolic growth

$$\boxed{v = \frac{D(\Delta C_0)^2}{2(C_\beta - C_e)(C_\beta - C_0)x}}$$

$$v \propto \underset{\text{Supersaturation}}{\Delta X_0} \propto \sqrt{(D/t)}$$

2) Diffusion Controlled lengthening of Plates or Needles

Diffusion Controlled lengthening:

$$\boxed{v = \frac{D\boxed{\Delta X_0}}{k(X_\beta - X_r)} \cdot \frac{1}{r}\boxed{\left(1 - \frac{r^*}{r}\right)}}$$

r ↑ ⟶ ΔX ↑

$v \rightarrow$ constant → $x \propto t$

Linear growth

3) Thickening of Plate-like Precipitates

Thickening of Plate-like Precipitates by Ledge Mechanism

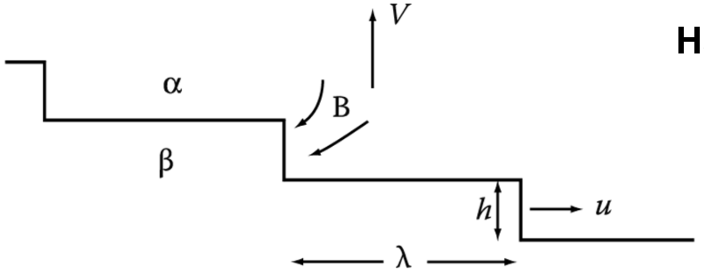

Half Thickness Increase

$$v = \frac{uh}{\lambda} \longrightarrow v = \frac{D\Delta X_0}{k(X_\beta - X_e)\lambda}$$

u : rate of lateral migration

Q1: Overall Transformation Kinetics–TTT diagram

“Johnson-Mehl-Avrami Equation”

5.4 Overall Transformation Kinetics – TTT Diagram

If isothermal transformation,

The fraction of Transformation as a function of Time and Temperature

$\rightarrow \; f(t,T)$

Plot f vs log t.

- isothermal transformation
- f ~ volume fraction of β at any time; 0~1

Plot the fraction of transformation (1%, 99%) in T-log t coordinate.

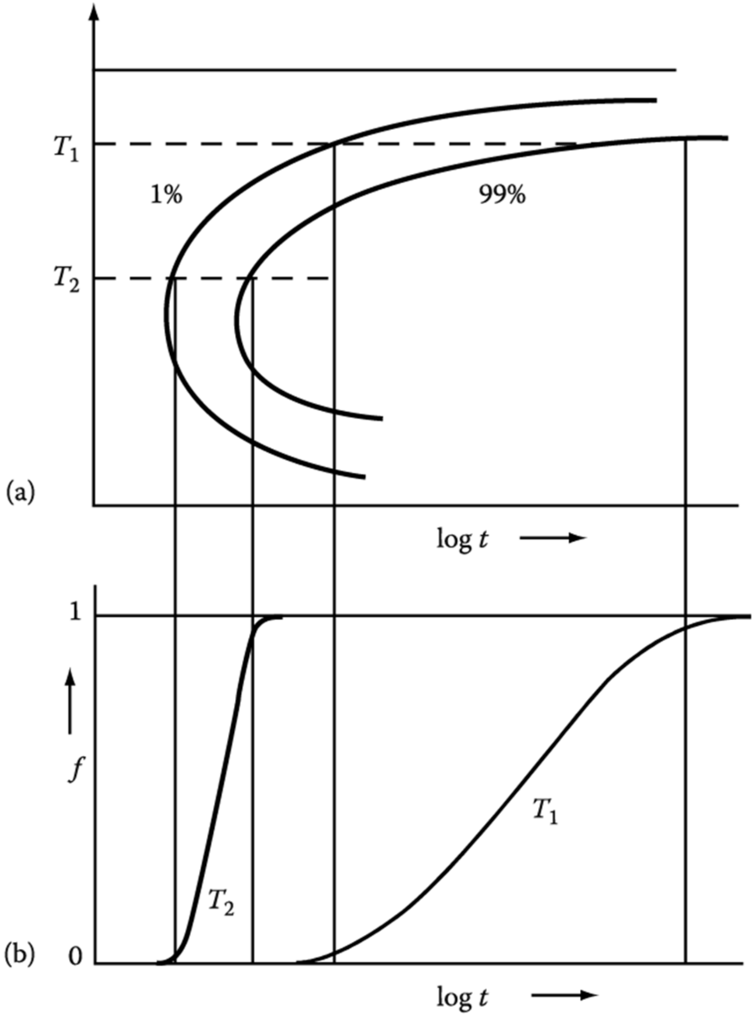

Fig. 5.23 The percentage transformation versus time for different transformation temperatures.

Time–Temperature–Transformation Curves (TTT)

- How much time does it take at any one temperature for a given fraction of the liquid to transform (nucleate and grow) into a crystal?

- $f(t,T) \sim \pi \underline{I(T)}\,\underline{\mu(T)^3}\, t^4/3$

where *f* is the fractional volume of crystals formed, typically taken to be 10^{-6}, a barely observable crystal volume.

Nucleation rates

$$I = n\nu \exp\left\{\left(\frac{16\pi\Delta H_{cryst}}{81RT}\right)\left(\frac{T_m}{\Delta T}\right)^2\right\}\exp\left\{\frac{-\Delta E_D}{RT}\right\}$$

Growth rates

$$\mu(T) = \left(\frac{fRT}{3N\pi a^2\eta(T)}\right)\left(1-\exp\left[\left(\frac{\Delta H_m}{RT}\right)\left(\frac{\Delta T}{T_m}\right)\right]\right)$$

Nucleation and Growth Rates – Poor Glass Formers

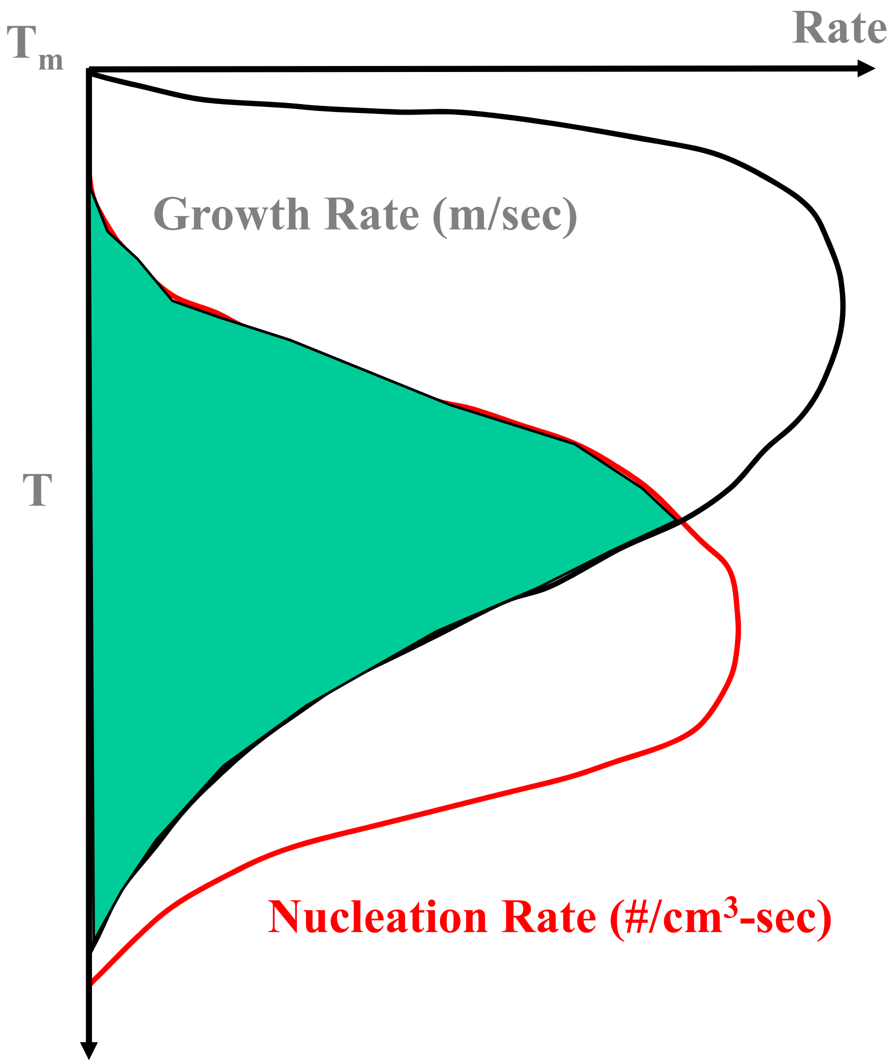

- **Strong overlap of growth and nucleation rates**
- **Nucleation rate is high**
- **Growth rate is high**
- **Both are high at the same temperature**

Nucleation and Growth Rates – Good Glass Formers

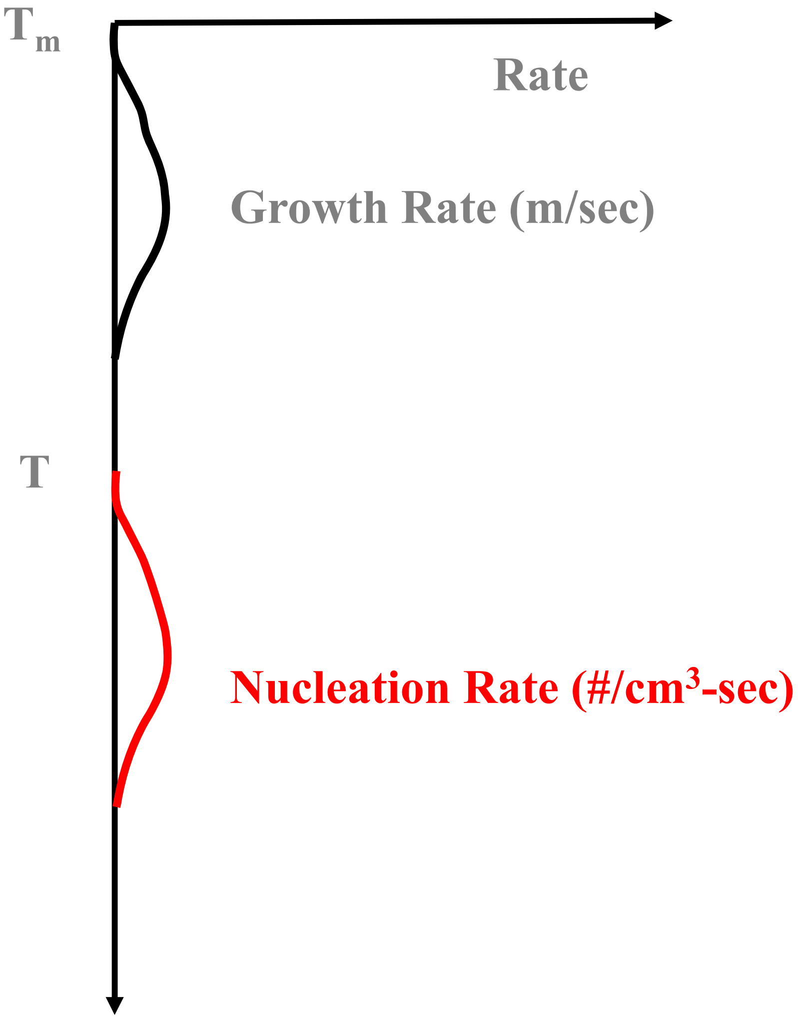

- **No overlap of growth and nucleation rates**
- Nucleation rate is small
- Growth rate is small
- At any one temperature one of the two is zero

* Time-Temperature-Transformation diagrams

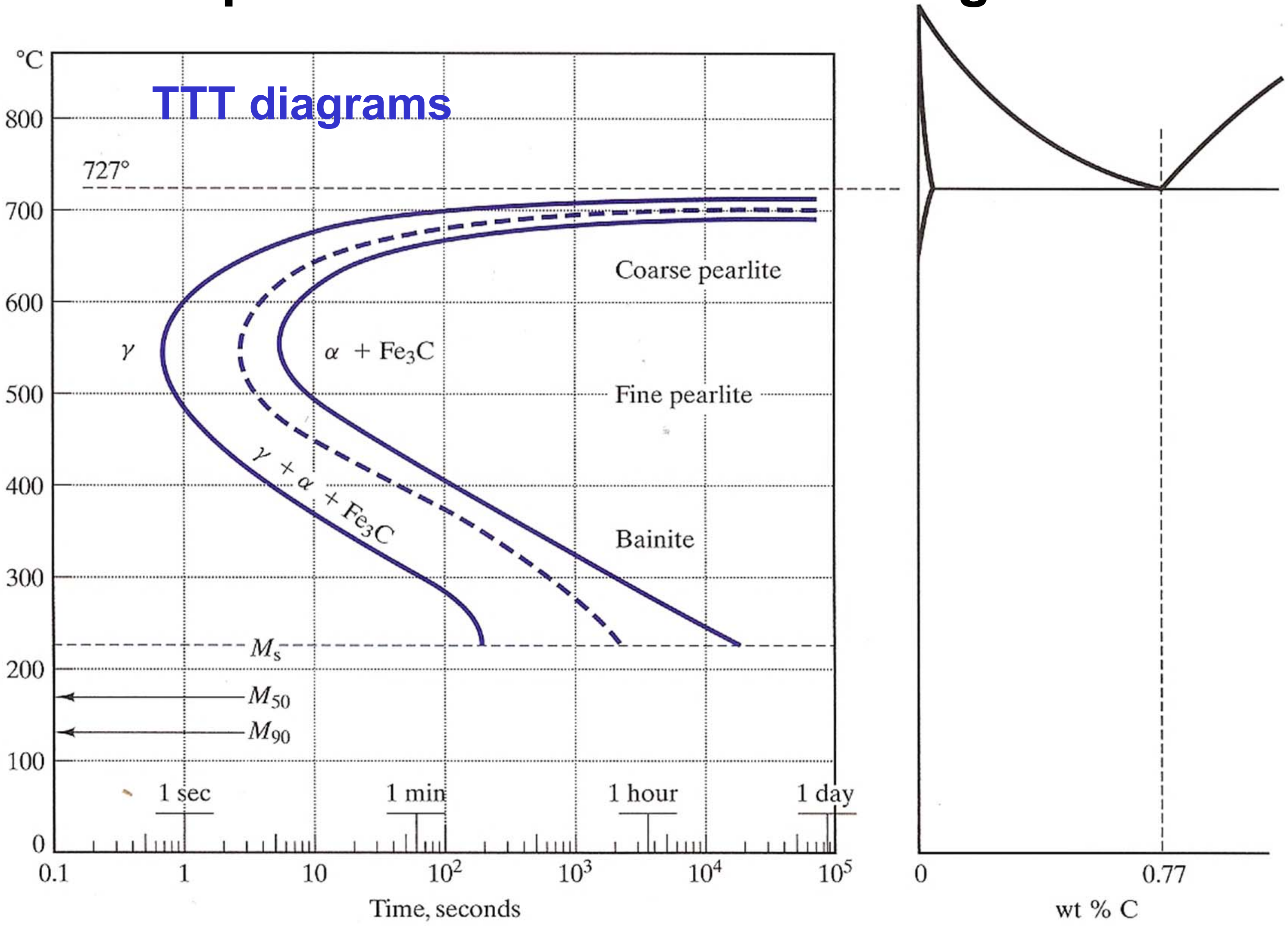

FIGURE 10.11 *A more complete TTT diagram for eutectoid steel than was given in Figure 10.7. The various stages of the time-independent (or diffusionless) martensitic transformation are shown as horizontal lines.* M_s *represents the start,* M_{50} *represents 50% transformation, and* M_{90} *represents 90% transformation. One hundred percent transformation to martensite is not complete until a final temperature* (M_f) *of* $-46°C$.

* Continuous Cooling Transformation diagrams

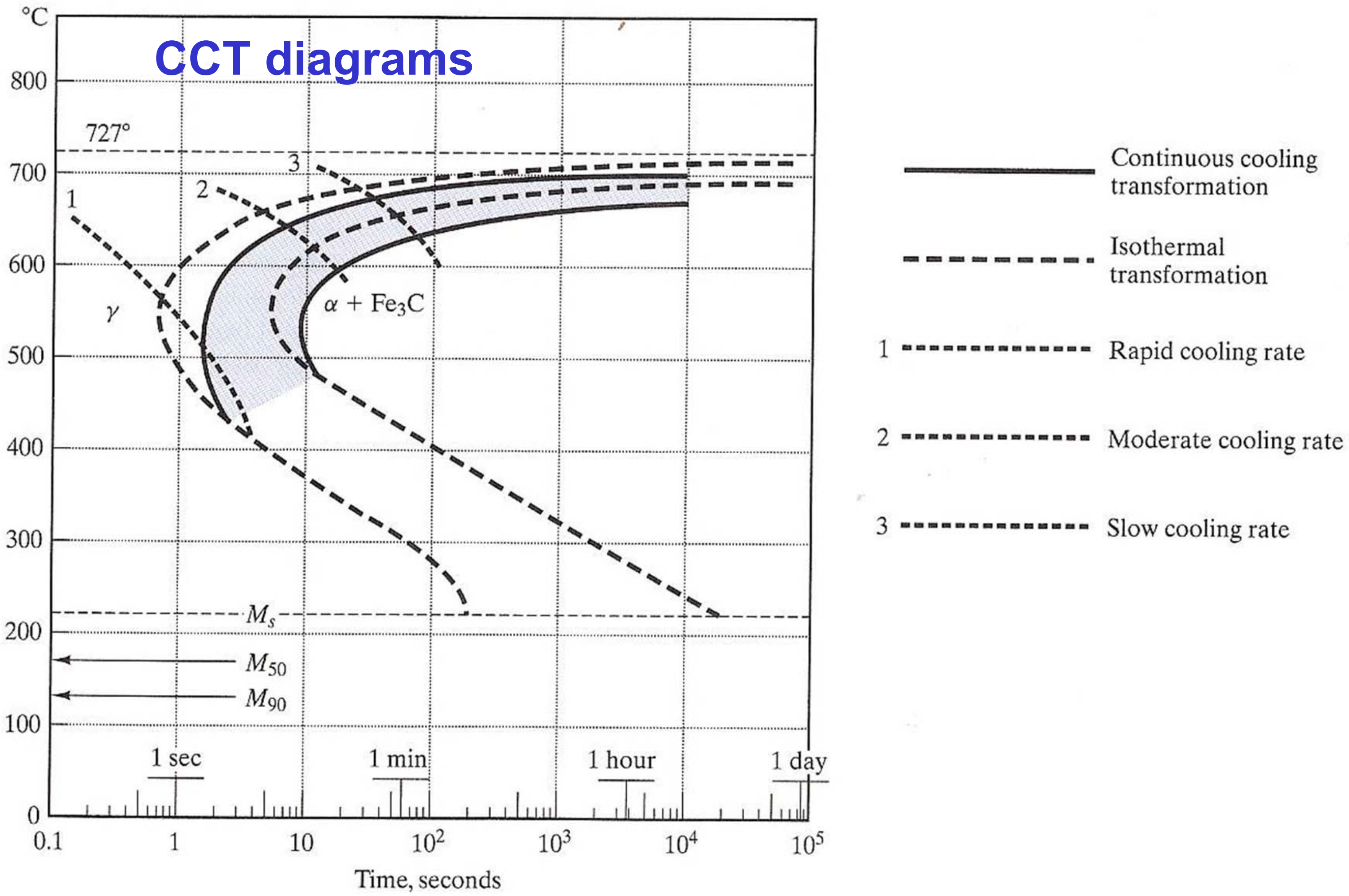

FIGURE 10.14 *A continuous cooling transformation (CCT) diagram is shown superimposed on the isothermal transformation diagram of Figure 10.11. The general effect of continuous cooling is to shift the transformation curves downward and toward the right.* (*After* Atlas of Isothermal Transformation and Cooling Transformation Diagrams, *American Society for Metals, Metals Park, OH, 1977.)*

Influence factors for $f(t,T)$: nucleation rate, growth rate, density and distribution of nucleation sites, impingement of adjacent cells

Example,

Three Transformation Types

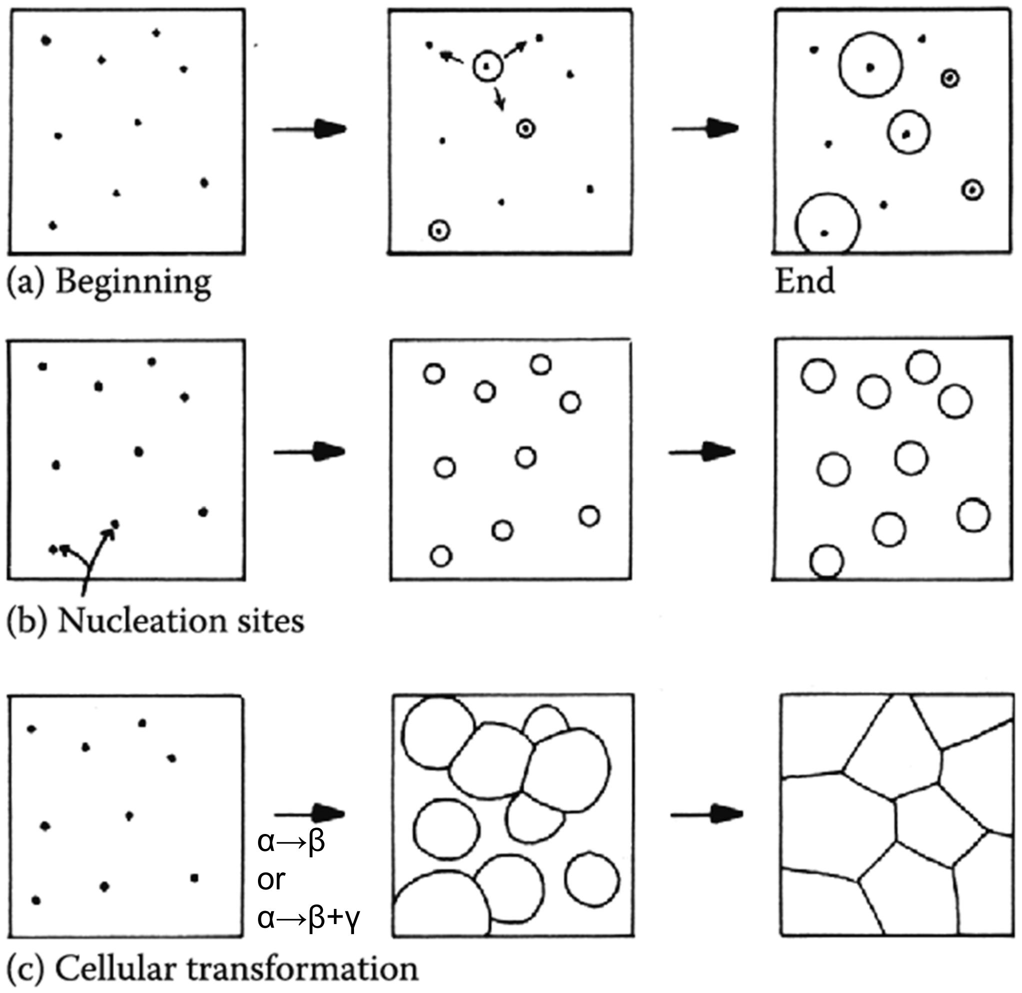

Wide range of particle sizes

Fig. 5.24 (a) Nucleation at a constant rate during the whole transformation.
(b) Site saturation – all nucleation occurs at the beginning of transformation.
(c) A cellular transformation.

(a) continuous nucleation

Metastable α phase with many nucleation sites by quenching to T_t

→ ***f*** **depends on the *nucleation rate and the growth rate.***

(b) all nuclei present at t = 0

→ ***f*** **depends on the *number of nucleation sites and the growth rate.***

(c) All of the parent phase is consumed by the transformation product.

Transformation terminate by the impingement of adjacent cells growing with a constant velocity.

→ **pearlite, cellular ppt, massive transformation, recrystallization**

α → β

Transformation Kinetics

- **Avrami proposed that for a three-dimensional nucleation and growth process kinetic law**

$$f = 1 - \exp\left(-kt^{n}\right)$$ Johnson-Mehl-Avrami equation

f : volume fraction transformed $= \dfrac{\text{Volume of new phase}}{\text{Volume of specimen}}$

- **Assumption :**
  - √ **reaction produces by nucleation and growth**
  - √ **nucleation occurs randomly throughout specimen**
  - √ **reaction product grows rapidly until impingement**

Constant Nucleation Rate Conditions

- Nucleation rate (I) is constant.
- Growth rate (v) is constant.
- No compositional change

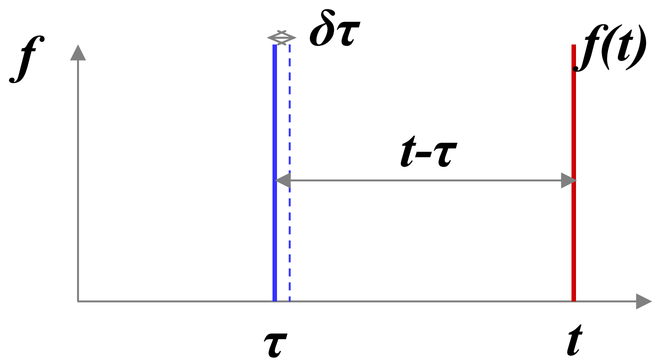

$$df_e = \frac{\begin{pmatrix}\text{Vol. of one particle nucleated}\\ \text{during } d\tau \text{ measured at time t}\end{pmatrix} \times \begin{pmatrix}\text{number of nuclei}\\ \text{formed during } d\tau\end{pmatrix}}{\text{Volume of specimen}}$$

$$df_e = \frac{\frac{4}{3}\pi[v(t-\tau)]^3 \times (IV_0 d\tau)}{V_0}$$

$$f_e(t) = \int_o^t I \cdot \frac{4}{3}\pi[v(t-\tau)]^3 d\tau$$

$$= I \cdot \frac{4}{3}\pi v^3 \left[-\frac{1}{4}(t-\tau)^4\right]_0^t = \boxed{\frac{1}{3}\pi I v^3 t^4}$$

$$V = \frac{4}{3}\pi r^3 = \frac{4}{3}\pi (vt)^3$$

$$V' = \frac{4}{3}\pi v^3 (t-\tau)^3$$

- do not consider impingement & repeated nucleation
- only true for $f \ll 1$

As time passes the β cells will eventually impinge on one another and the rate of transformation will decrease again.

Constant Nucleation Rate Conditions

- consider impingement + repeated nucleation effects

$$df = (1-f)\,df_e \longrightarrow df_e = \frac{df}{1-f}$$

$$f_e = -\ln(1-f)$$

$$f(t) = 1-\exp(-f_e(t)) = 1-\exp\left(-\frac{\pi}{3}Iv^3t^4\right)$$

* Short time:
1-exp(z)~Z (z ≪1)

* Long time:
t→∞, $f \rightarrow 1$

Johnson-Mehl-Avrami Equation

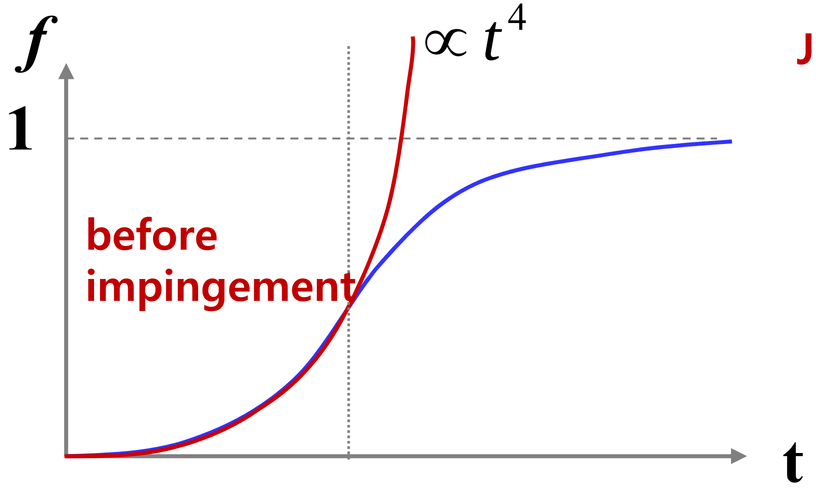

$$f = 1-\exp(-kt^n)$$

***k*:** *T* sensitive ***f*(*I*, *v*)** $\quad -\frac{\pi}{3}Iv^3$

***n*:** **1 ~ 4** (depend on nucleation mecnanism)

Growth controlled. Nucleation-controlled.

If no change of nucleation mechanism during phase transformation, n is not related to T.

i.e. 50% transform

Exp (-0.7) = 0.5

$$kt_{0.5}^n = 0.7 \qquad t_{0.5} = \frac{0.7}{k^{1/n}} \xrightarrow{\frac{\pi}{3}Iv^3} t_{0.5} = \frac{0.9}{N^{1/4}v^{3/4}}$$

Rapid transformations are associated with (large values of k), or (rapid nucleation and growth rates)

5.4 Overall Transformation Kinetics

If isothermal transformation,

The fraction of Transformation as a function of Time and Temp. → f (t,T)

TTT Diagram ⟺ CCT Diagram

*** Constant Nucleation Rate Conditions**

$$f(t) = 1 - \exp\left(-f_e(t)\right) = 1 - \exp\left(-\frac{\pi}{3} I v^3 t^{4}\right)$$

*** Short time:**
1-exp(z)~Z (z ≪1)

*** Long time:**
t→∞, f→1

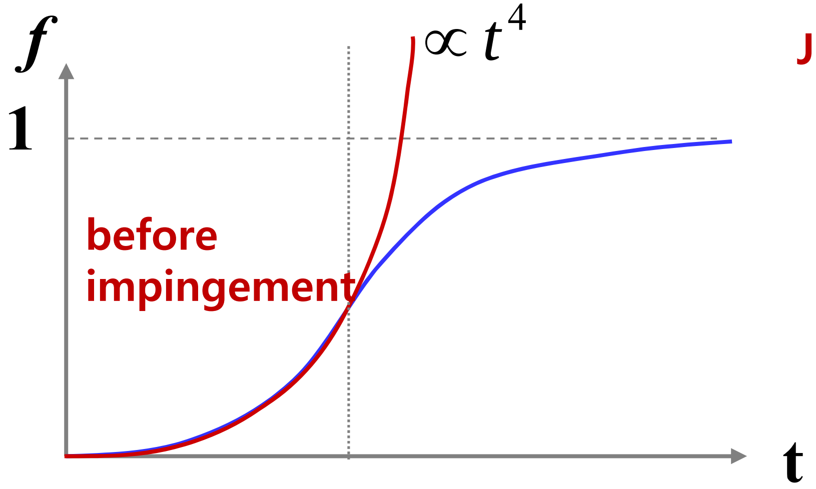

Johnson-Mehl-Avrami Equation

$$f = 1 - \exp\left(-kt^n\right)$$

k: T sensitive $f(I, v)$ $-\frac{\pi}{3} I v^3$

n: 1 ~ 4 (depend on nucleation mecnanism)

Growth controlled. **Nucleation-controlled.**

If no change of nucleation mechanism during phase transformation, n is not related to T.

i.e. 50% transform

Exp (-0.7) = 0.5

$$kt_{0.5}^n = 0.7 \quad t_{0.5} = \frac{0.7}{k^{1/n}} \quad \xRightarrow{\frac{\pi}{3} I v^3} \quad t_{0.5} = \frac{0.9}{I^{1/4} v^{3/4}}$$

Rapid transformations are associated with (large values of k), or (rapid nucleation and growth rates)

Q2: Precipitation in Age-Hardening Alloys

The theory of nucleation and growth can provide general guidelines for understanding civilian transformation.

5.5 Precipitation in Age-Hardening Alloys

Table 5.2 Some precipitation-Hardening Sequences

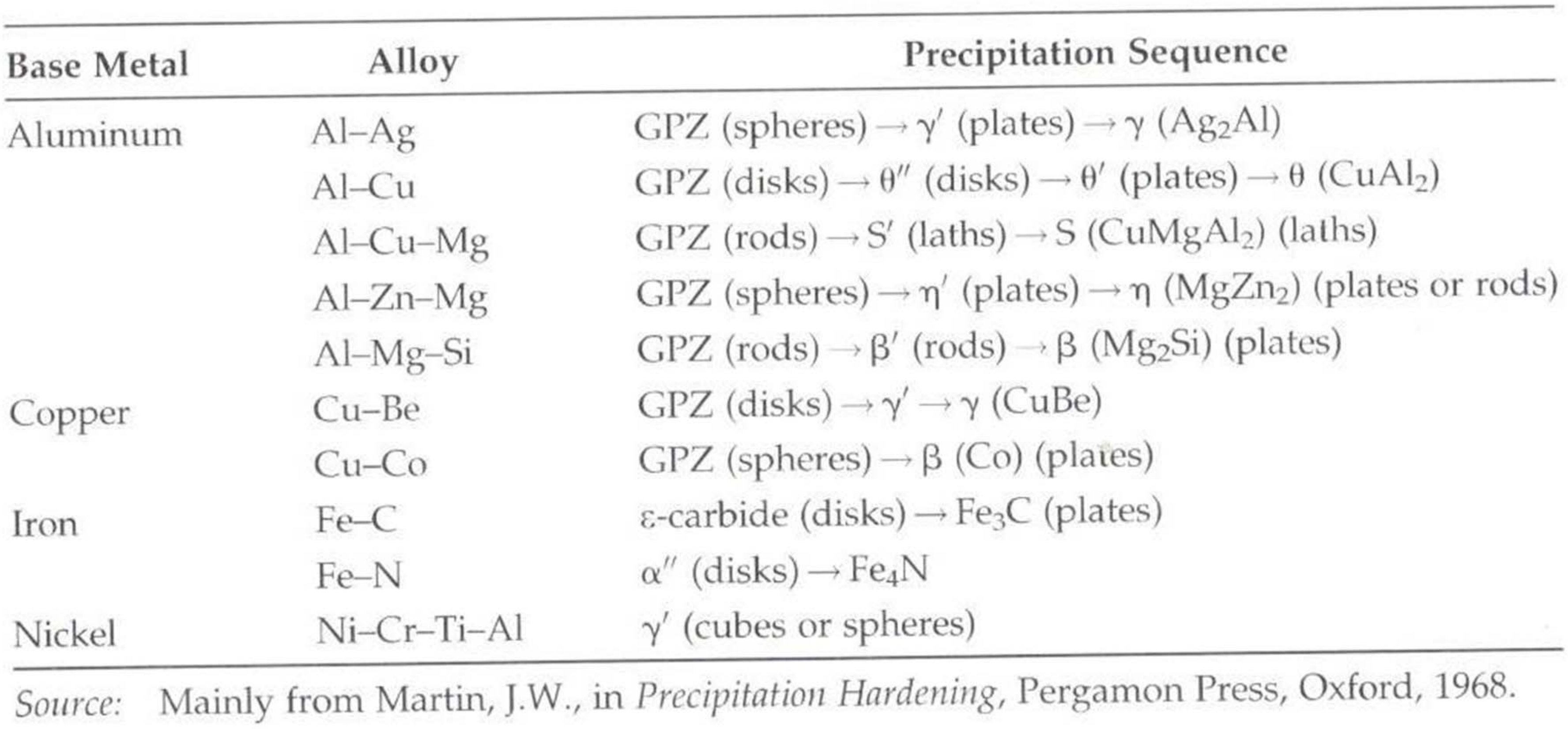

Base Metal	Alloy	Precipitation Sequence
Aluminum	Al–Ag	GPZ (spheres) $\rightarrow \gamma'$ (plates) $\rightarrow \gamma$ (Ag_2Al)
	Al–Cu	GPZ (disks) $\rightarrow \theta''$ (disks) $\rightarrow \theta'$ (plates) $\rightarrow \theta$ ($CuAl_2$)
	Al–Cu–Mg	GPZ (rods) $\rightarrow S'$ (laths) $\rightarrow S$ ($CuMgAl_2$) (laths)
	Al–Zn–Mg	GPZ (spheres) $\rightarrow \eta'$ (plates) $\rightarrow \eta$ ($MgZn_2$) (plates or rods)
	Al–Mg–Si	GPZ (rods) $\rightarrow \beta'$ (rods) $\rightarrow \beta$ (Mg_2Si) (plates)
Copper	Cu–Be	GPZ (disks) $\rightarrow \gamma' \rightarrow \gamma$ (CuBe)
	Cu–Co	GPZ (spheres) $\rightarrow \beta$ (Co) (plates)
Iron	Fe–C	ε-carbide (disks) $\rightarrow Fe_3C$ (plates)
	Fe–N	α'' (disks) $\rightarrow Fe_4N$
Nickel	Ni–Cr–Ti–Al	γ' (cubes or spheres)

Source: Mainly from Martin, J.W., in *Precipitation Hardening*, Pergamon Press, Oxford, 1968.

Let us now turn to a consideration of some examples of the great variety of civilian transformations in solid.

5.5 Precipitation in Age-Hardening Alloys

Precipitation in Aluminum-Copper Alloys

Al-4 wt%Cu (1.7 at %)

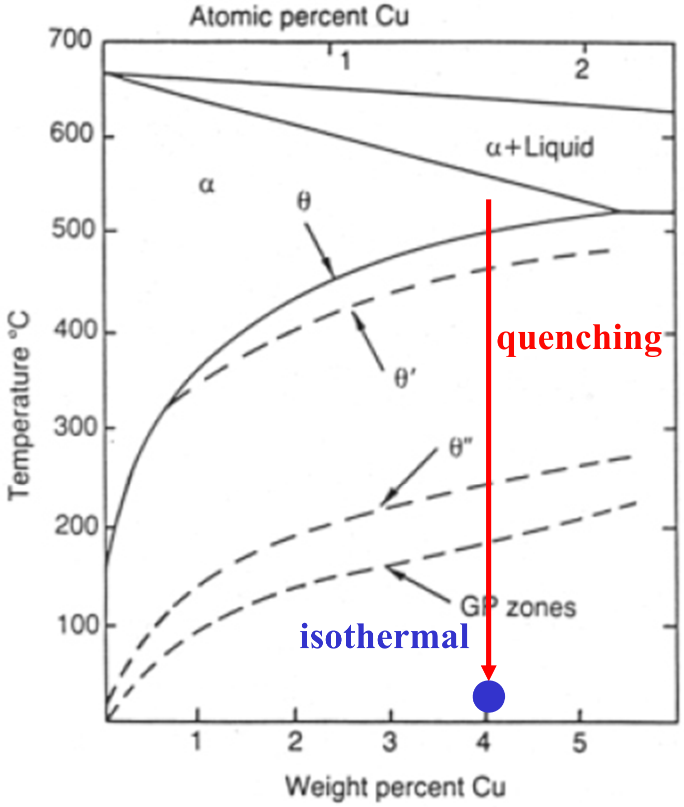

Fig. 5.25 Al-Cu phase diagram showing the metastable GP zone, Θ″ and Θ′ solvuses. (Reproduced from G. Lorimer, *Precipitation Processes in Solids*, K.C. Russell and H.I. Aaronson (Eds.), The Metallurgical Society of AMIE, 1978, p. 87.)

$\boxed{\alpha_0}$ **540°C heat treatment → Quenching + Isothermal (below 180°C)**

Supersaturated solid solution

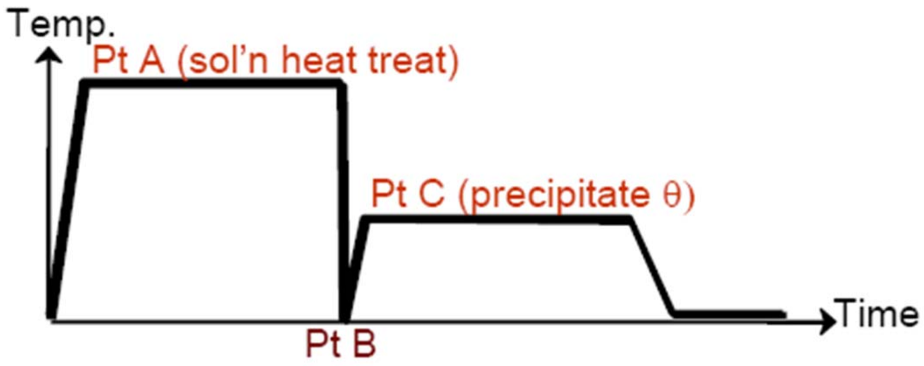

$\rightarrow \alpha_1$**+GP zones**

$\rightarrow \alpha_2 + \theta'' \rightarrow \alpha_3 + \theta' \rightarrow \alpha_4 + \theta$

($CuAl_2$)

In most system, α, β phase~ different crystal structure → incoherent nuclei with large γ ~ impossible to homogeneous nucleation of β → Homogeneous nucleation of metastable phase β′ (GP Zones, Section 5.5.1)

Driving force for GP zone precipitation

$$\boxed{\Delta G_{\theta}^{*} > \underline{(\Delta G_V - \Delta G_s)} >> \Delta G_{zone}^{*}}$$

5.5.1 GP Zones

The zones minimize their strain energy by choosing a disc-shape perpendicular to the elastically soft <100> directions in the fcc matrix (as shown in Fig. 5.26).

2 atomic layers thick and 10 nm in diameter with a spacing of ~10 nm

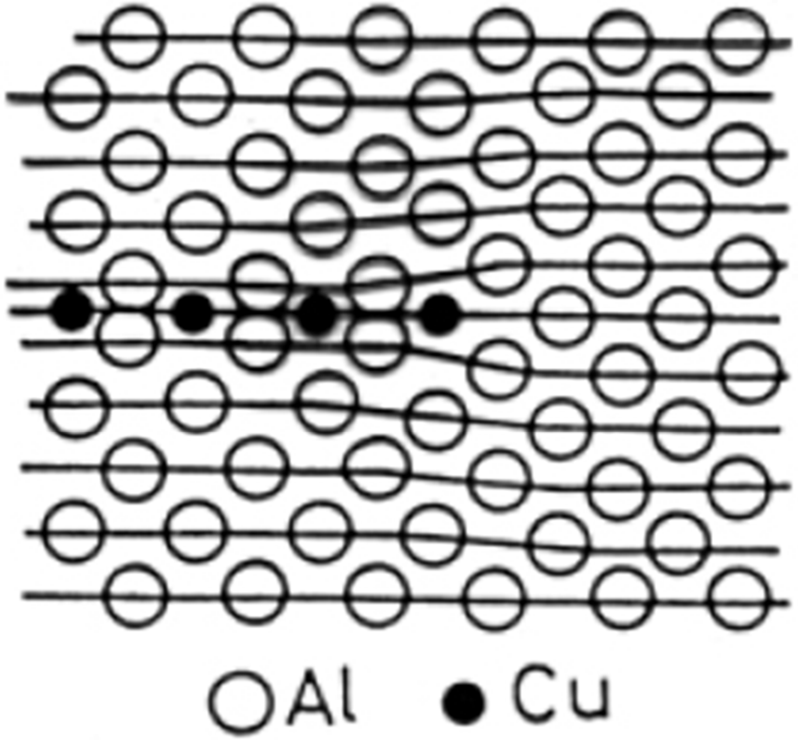

Fully coherent Cu-rich area
with very low interfacial E

Fig. 5.26 Section through a GP zone parallel to the (200) plane. (Based on the work of V. Gerold: *Zeitschrift für Metallkunde* **45** (1954) 599.)

: 이러한 응집체는 완전한 석출 입자로 볼 수 없으며, 때때로 석출대 (zone)로 명명함.

The zone appear to be homogeneously nucleated, however, excess vacancies are thought to play an important role in their formation (be returned to later)

GP zones of Al-Cu alloys (x 720,000, TEM)

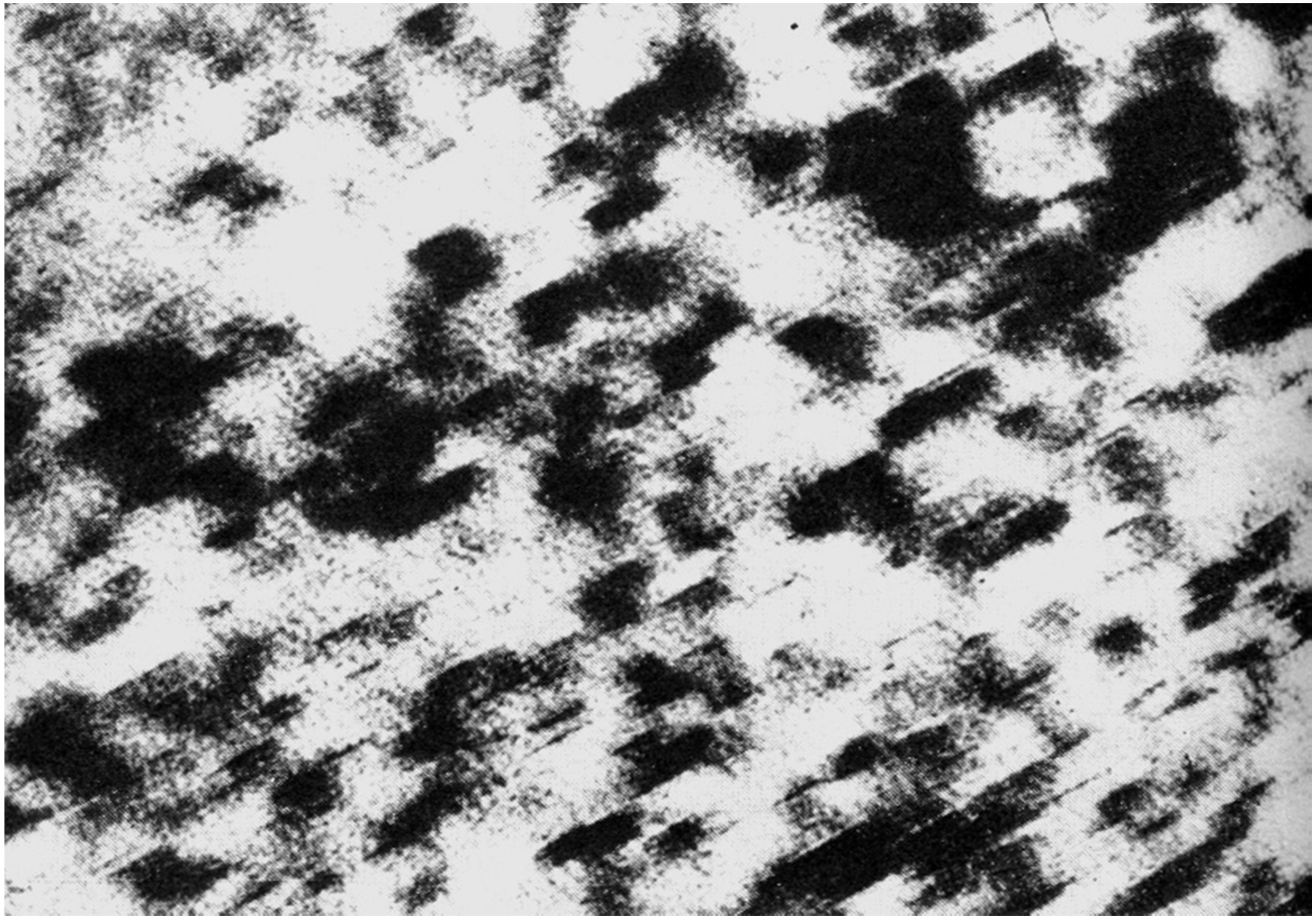

Fully coherent, about 2 atomic layers thick and

10 nm in diameter with a spacing of ~ 10 nm

: The contrast in the image is due to the coherency misfit strain perpendicular to the zones.

(Coherency misfit strain→local variations in the intensity of electron diffraction→image contrast change)

Transition phases

$\alpha_0 \rightarrow \alpha_1$ **+GP zone** $\rightarrow \alpha_2 + \theta'' \rightarrow \alpha_3 + \theta' \rightarrow \alpha_4 + \theta$ **(CuAl$_2$)**

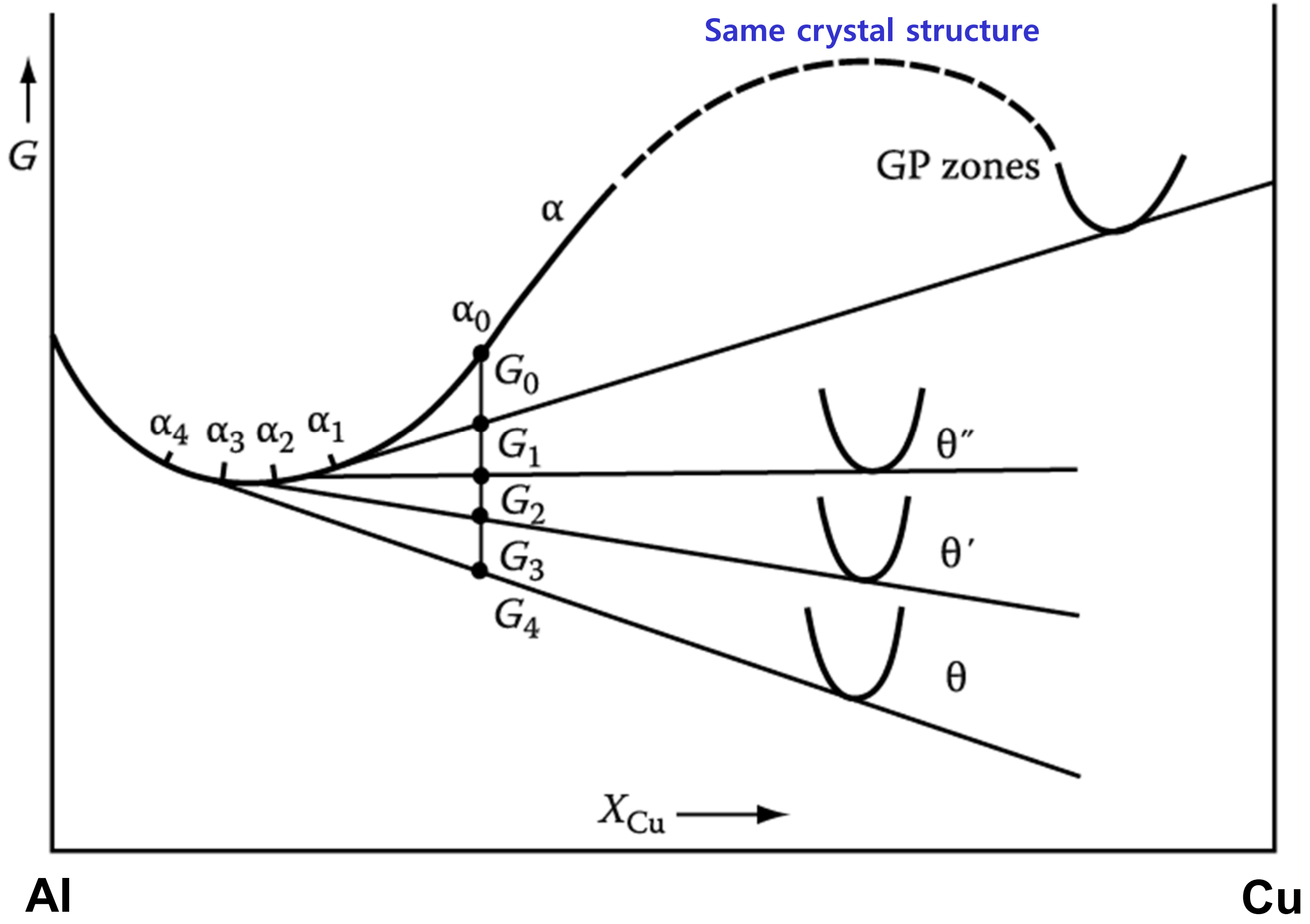

Fig. 5.27 A schematic molar free energy diagram for the Al-Cu system.

$\alpha_0 \rightarrow \alpha_1$+GP zone→$\alpha_2+\theta''$ →$\alpha_3+\theta'$ →$\alpha_4+\theta$ (CuAl$_2$)

Low Activation Energy of Transition Phases

➡ ∵ the crystal structures of the transition phases are intermediate between those of the matrix and the equilibrium phase.

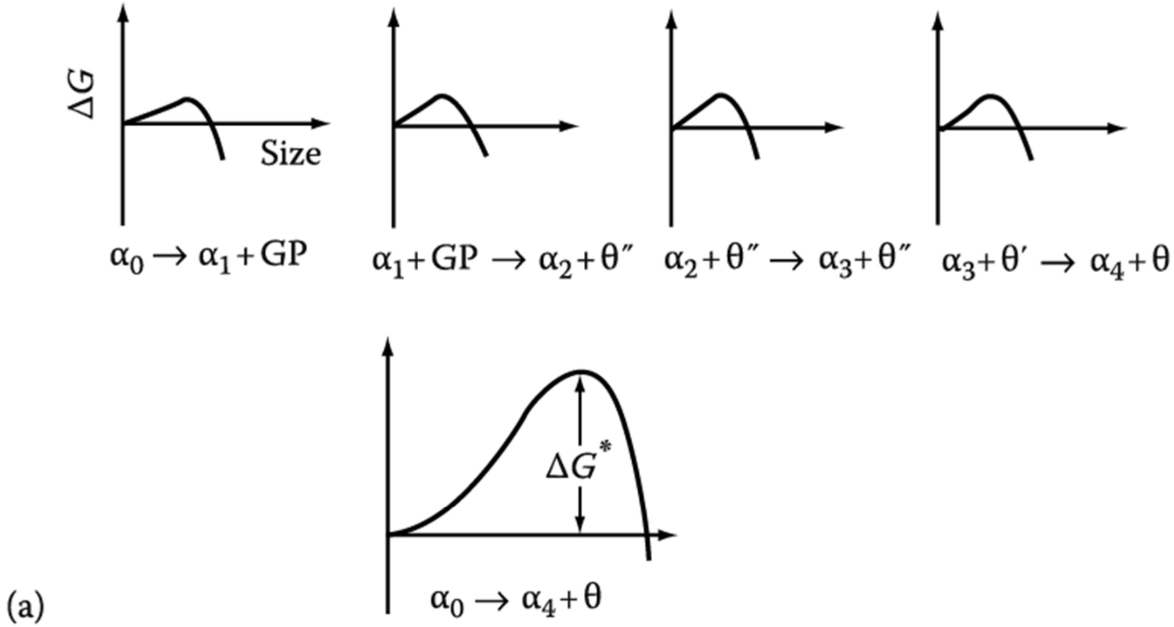

Transition phases (중간상, θ″ & θ′): a high degree of coherence, low interfacial E contribution to min ΔG*.

Equilibrium phase (평형상, θ): complex crystal structure that is incompatible with the matrix → high E interfaces and high ΔG*.

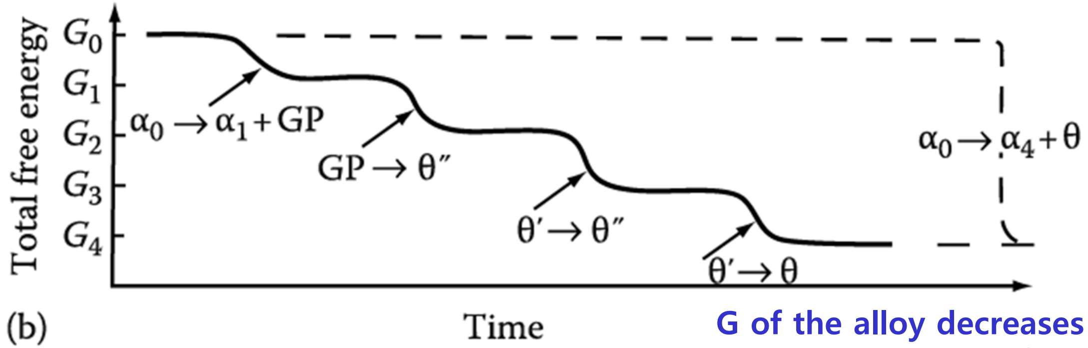

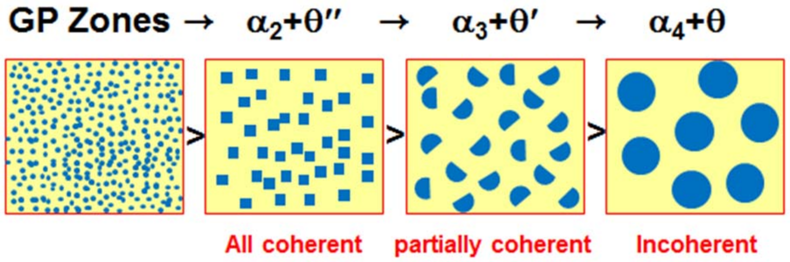

G of the alloy decreases more rapidly via the transition phases than by direct transformation to the equilibrium phase.

(a) The activation E barrier to the formation of each transition phase is very small in comparison to the barrier against the direct precipitation of the equilibrium phase. (b) Schematic diagram showing the total free E of the alloy versus time.

The Crystal Structures of θ″, θ′ and θ

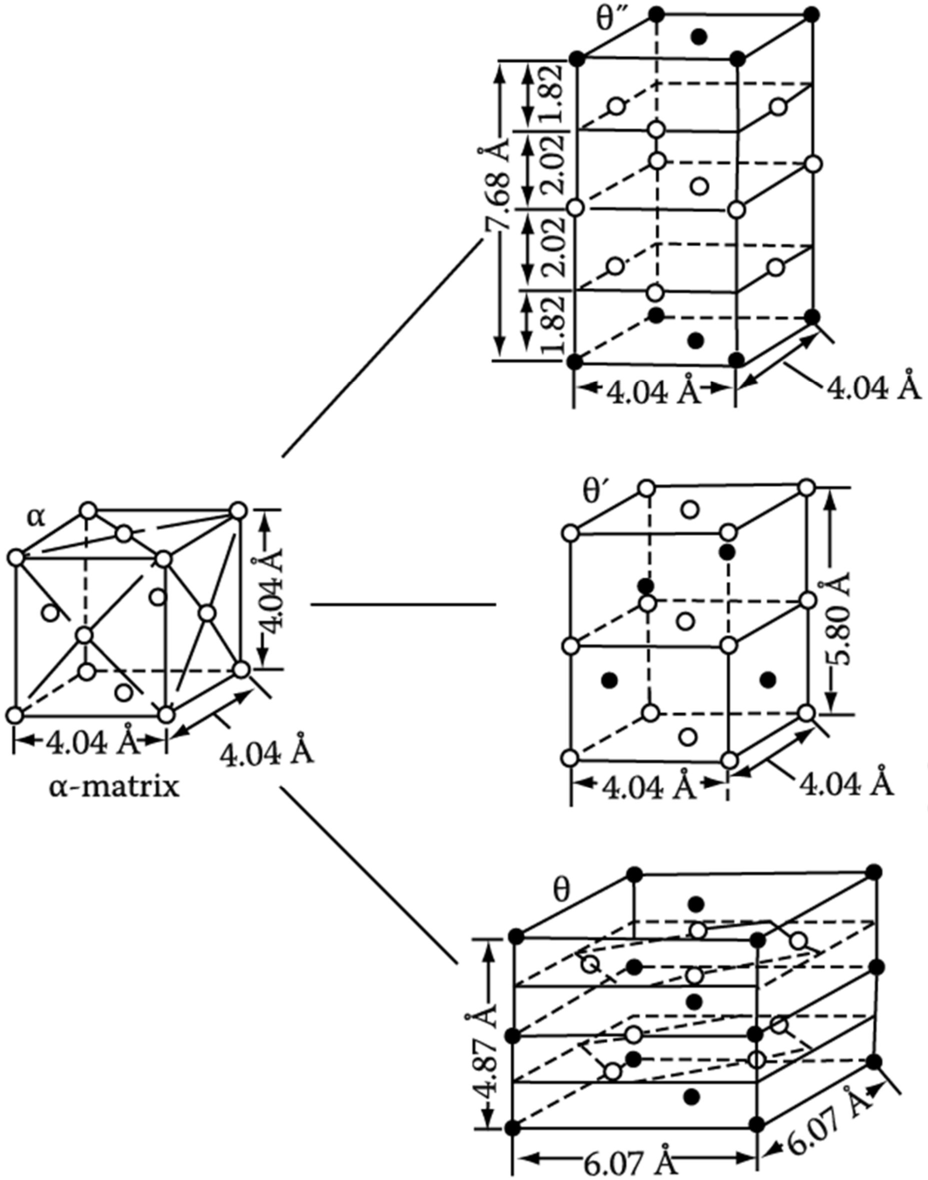

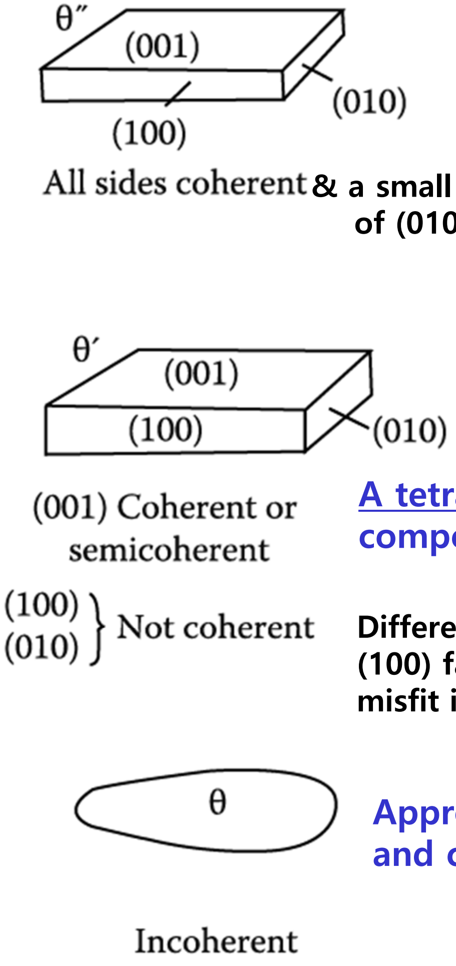

A tetragonal unit cell (= a distorted fcc structure in which the Cu and Al atoms are ordered on (001) planes.)

& a small distortion in the [001] direction of (010) and (100) faces

A tetragonal with an approximate composition $CuAl_2$

Different crystal structure in (010) and (100) faces to the matrix and a large misfit in the [001] direction

Approximate composition $CuAl_2$ and complex BCT structure

Fig. 5.29 Structure and morphology of θ'', θ' and θ in Al-Cu (○ Al. ● Cu).

θ″ of Al-Cu alloys (x 63,000, TEM)

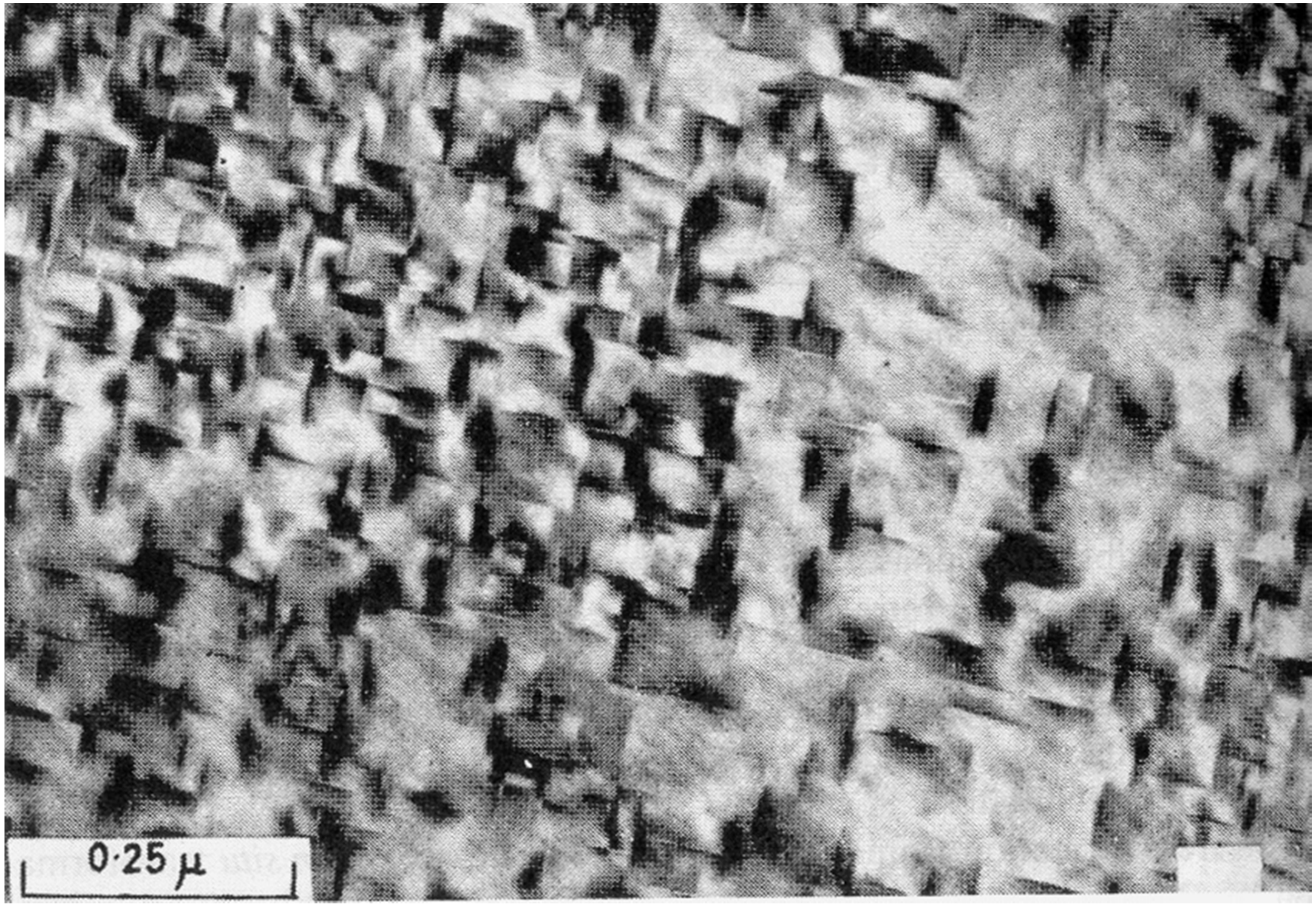

Tetragonal unit cell, essentially a distorted fcc in which Cu and Al atoms are ordered on (001) planes, fully-coherent plate-like ppt with $\{001\}_\alpha$ habit plane. ~ 10 nm thick and 100 nm in diameter (larger than GP zones).

: Like the GP zones, the θ″ precipitates are visible by virtue of the coherency-strain fields caused by the misfit perpendicular to the plates.

θ′ of Al-Cu alloys (x 18,000, TEM)

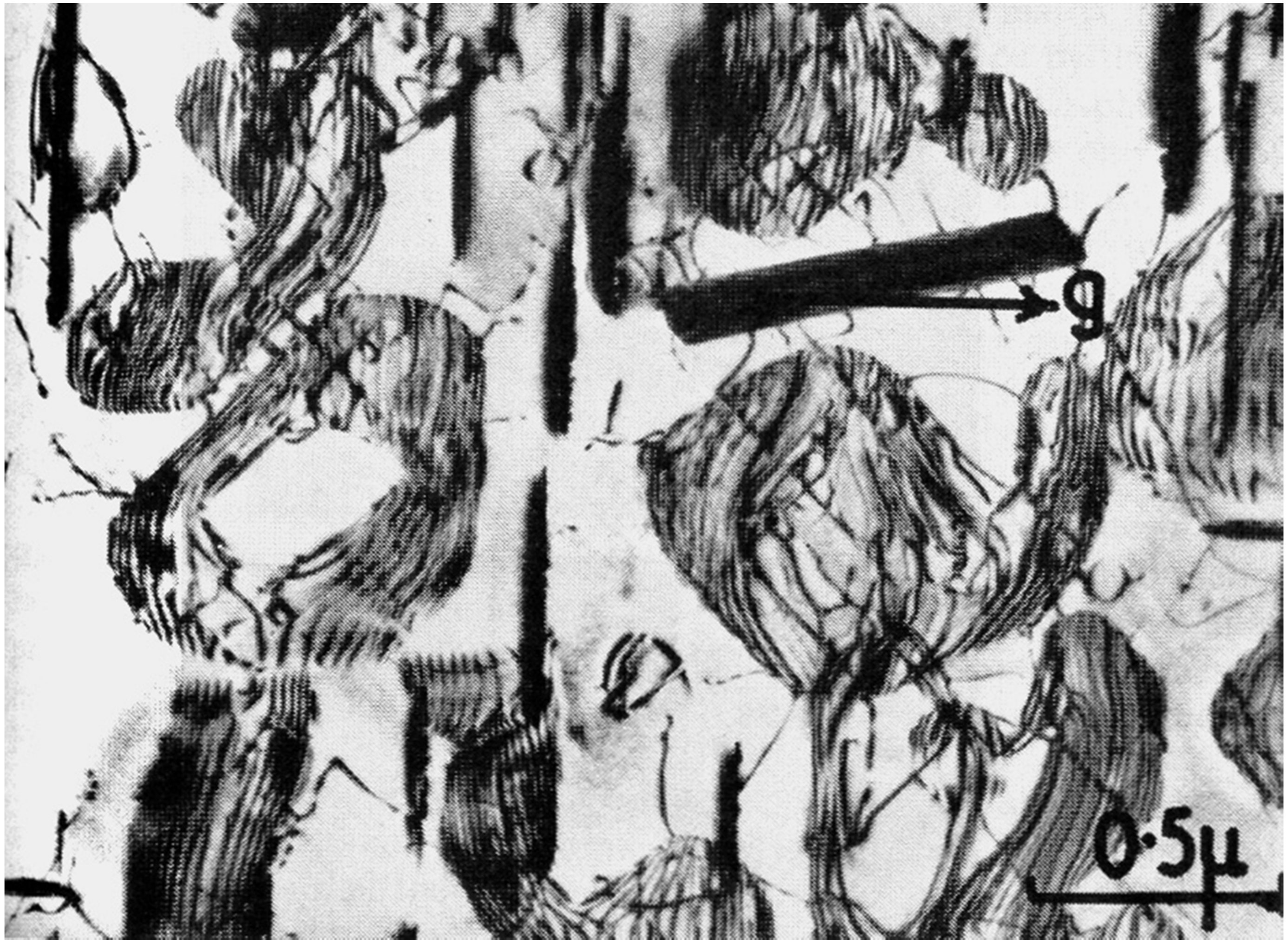

θ′ has (001) planes that are identical with $\{001\}_\alpha$ and forms as plates on $\{001\}_\alpha$ with the same orientation relationship as θ″.
But, (100), (010) planes → incoherent, ~ 1 μm in diameter.

: The broad faces of the plates are initially fully coherent but lose coherency as the plates grow, while the edges of the plates are either incoherent or have a complex semicoherent structure.

θ of Al-Cu alloys x 8,000

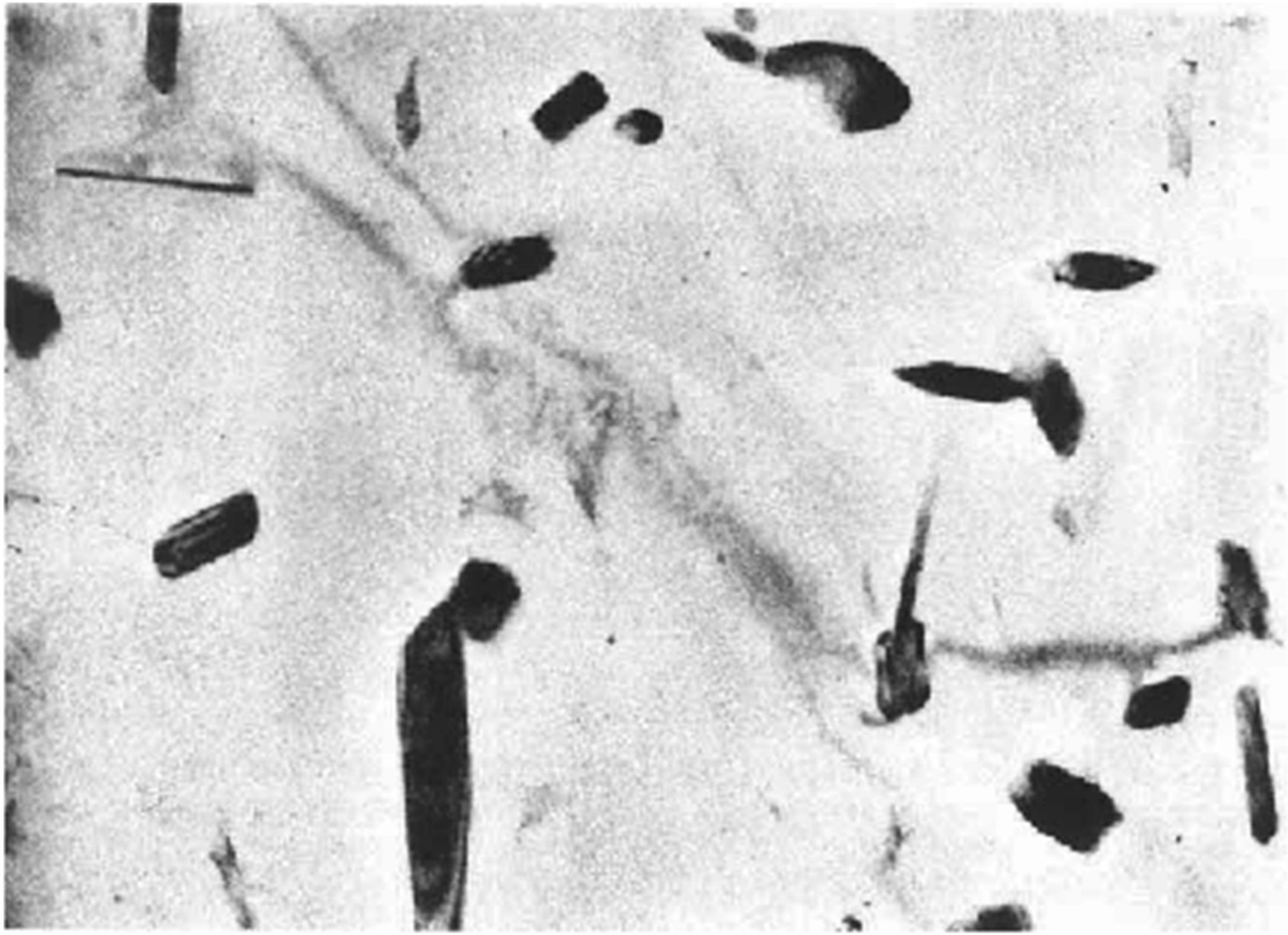

$CuAl_2$: complex body centered tetragonal, incoherent or complex semicoherent

: large size and coarse distribution of the precipitates

Nucleation sites

in Al-Cu alloys

(0) GP zones → θ'':

GP zones

~ very potent nucleation sites for θ''

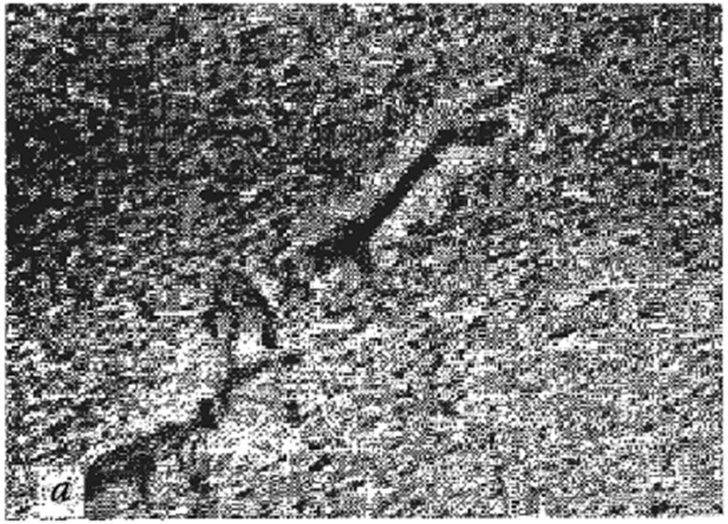

(a) **$\theta'' \rightarrow \theta'$. θ' nucleates at dislocation (x 70,000).**

: Dislocation can reduce the misfit in two <100> matrix directions.

As the θ' grows the surrounding, less-stable θ'' phase can be seen to dissolve.

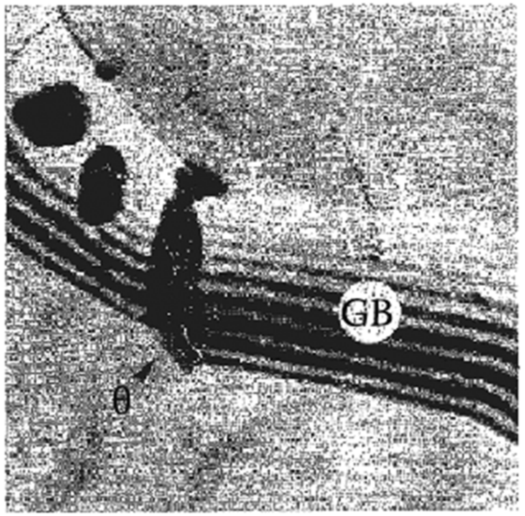

(b) **θ nucleation on grain boundary (GB)(x 56,000)**

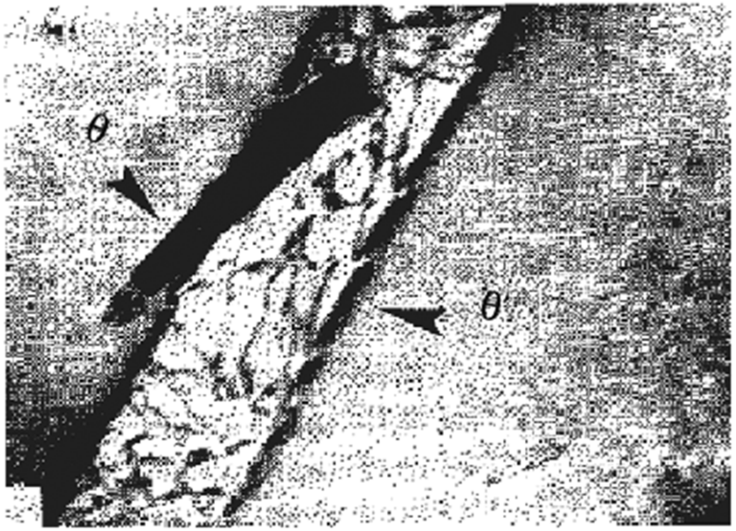

(c) **$\theta' \rightarrow \theta$. θ nucleates at θ'/matrix interface (x 70,000).**

: governed by the need to reduce the large interfacial energy contribution to ΔG^* for this phase

Fig. 5.31 Electron micrographs showing nucleation sites in Al-Cu alloys.

* Effect of Aging Temperature on the Sequence of Precipitates

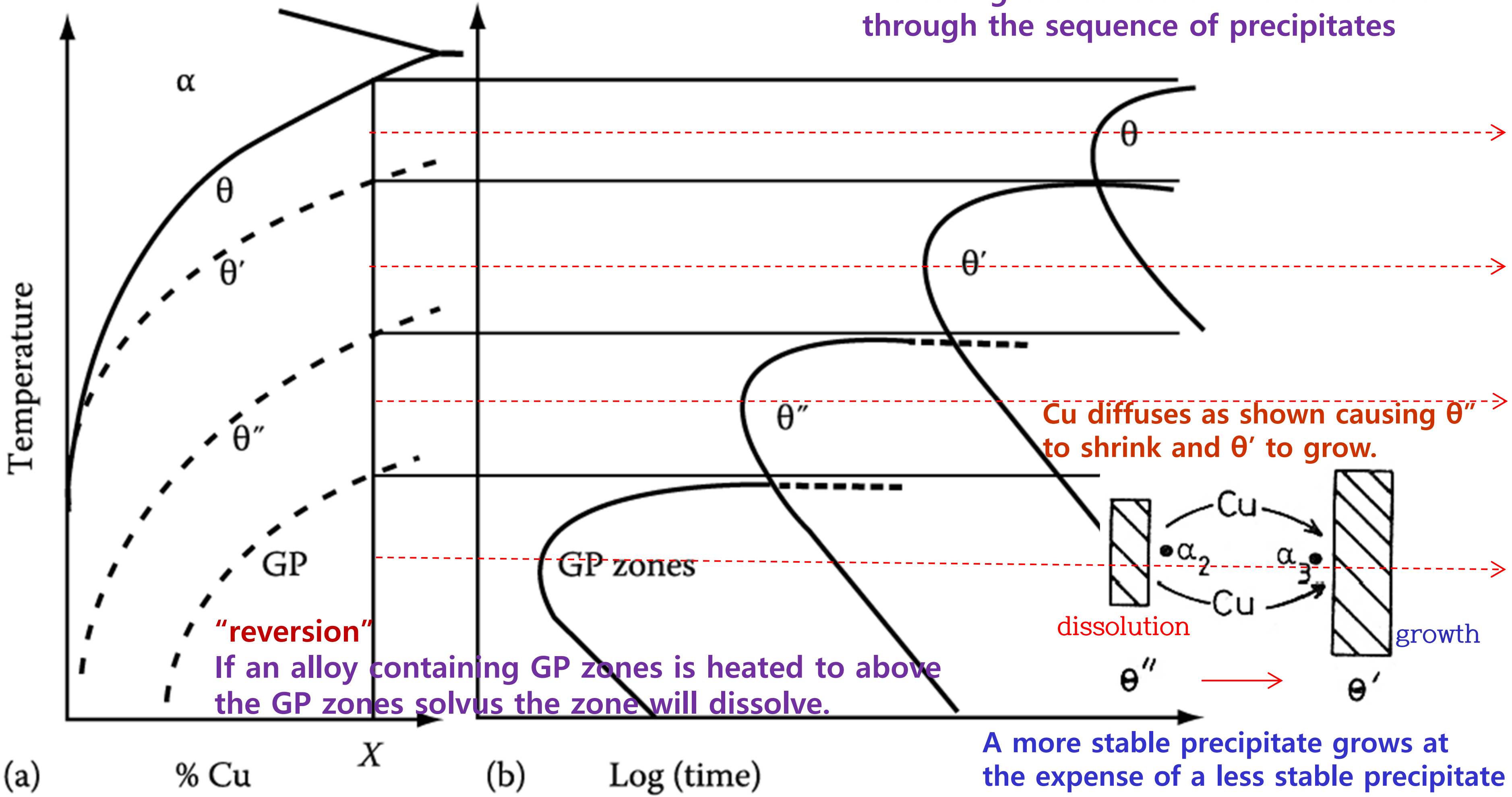

Increasing coarseness of microstructure through the sequence of precipitates

Cu diffuses as shown causing θ″ to shrink and θ′ to grow.

"reversion"
If an alloy containing GP zones is heated to above the GP zones solvus the zone will dissolve.

A more stable precipitate grows at the expense of a less stable precipitate
(석출순서에 따라 미세조직의 조대화 발생)

Fig. 5.32 (a) Metastable solvus lines in Al-Cu (schematic).
(b) Time for start of precipitation at different temperatures for alloy X in (a).

Q3: Quenched-in vacancies vs Precipitate-free zone

5.5.3. Quenched-in Vacancies

If $X_v < X_v^c$ critical vacancy supersaturation,
Precipitate nucleation X → formation of PFZ

a) Excess Ⓥ→ Ⓓ nucleation and moving ↑:
Heterogeneous nucleation sites ↑

b) Excess Ⓥ → atomic mobility ↑ at ageing temp:
speeds up the process of nucleation and growth

ex) rapid formation of GP zones at the relatively low aging temperature. (possible to RT aging in Al-Cu alloy)

In the vicinity of grain boundaries on subsequent aging,

a) Precipitate-Free Zone(PFZ) due to Vacancy Diffusion during quenching

Solute concentration within the zone ~ largely unchanged, but no precipitate at GB
∵ a critical vacancy supersaturation must be exceeded for nucleation to occur.

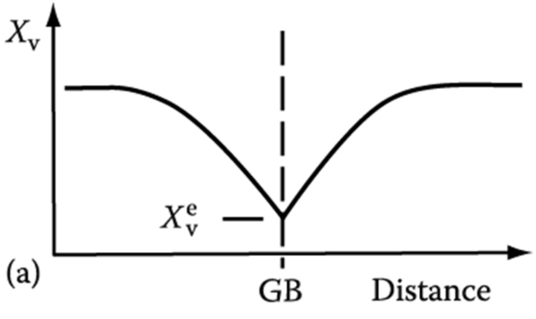

Similar PFZs can also form at inclusions and dislocations.

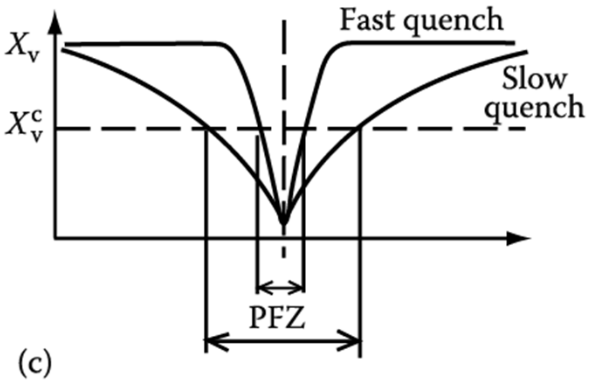

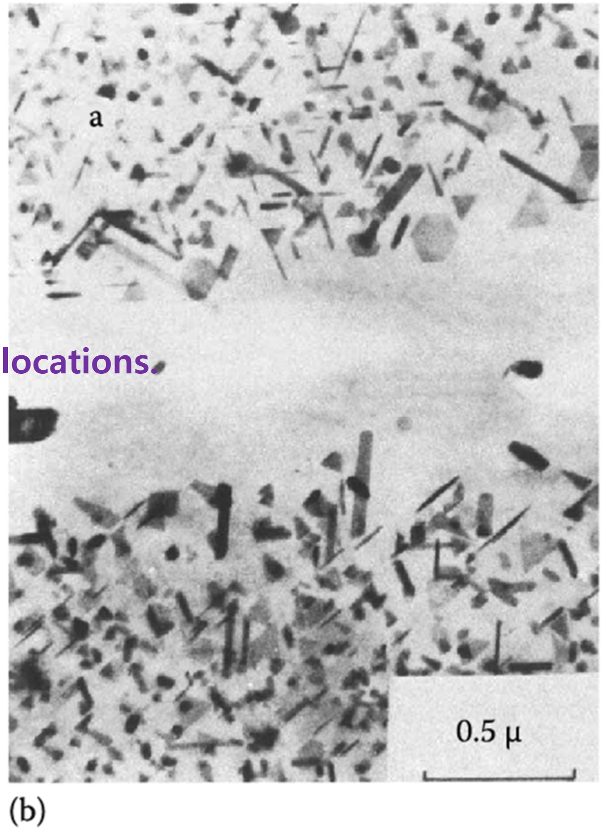

Fig. 5.35 A PFZ due to vacancy diffusion to a grain boundary during quenching.
(a) Vacancy concentration profile. (b) A PFZ in an Al-Ge alloy (x 20,000)
(c) Dependence of PFZ width on critical vacancy concentration X_v^c and rate of quenching.

* Equilibrium Vacancy Concentration

at equilibrium $$\left(\frac{dG}{dX_V}\right)_{X_V = X_V^e} = 0$$

$$\Delta H_V - T\Delta S_V + RT \ln X_V^e = 0$$

A constant ~3, independent of T   Rapidly increases with increasing T

$$X_V^e = \boxed{\exp\frac{\Delta S_V}{R}} \cdot \exp\frac{-\Delta H_V}{RT}$$

putting $\Delta G_V = \Delta H_V - T\Delta S_V$

$$\boxed{X_V^e = \exp\frac{-\Delta G_V}{RT}}$$

increases exponentially with increasing T

- **In practice, ΔH_V is of the order of 1 eV per atom and X_V^e reaches a value of about 10^{-4}~10^{-3} at the melting point of the solid**

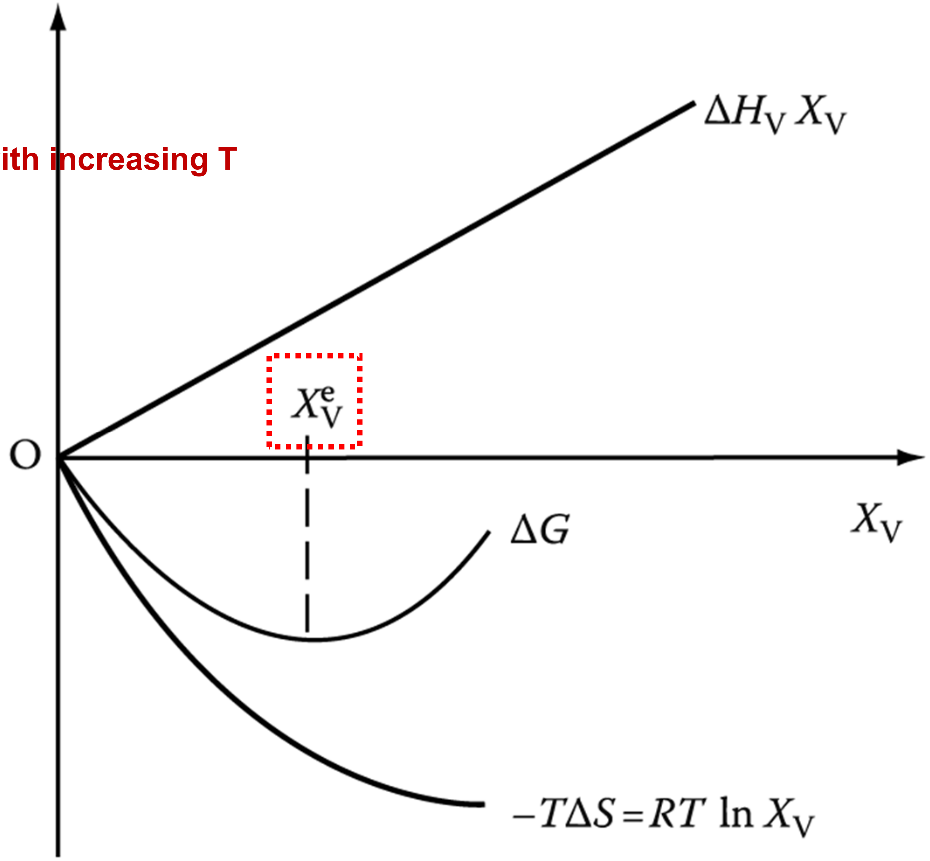

Fig. 1.37 Equilibrium vacancy concentration.

: adjust so as to reduce G to a minimum

b) Another cause of PFZs can be the nucleation and growth of GB precipitates during cooling from the solution treatment temperature.

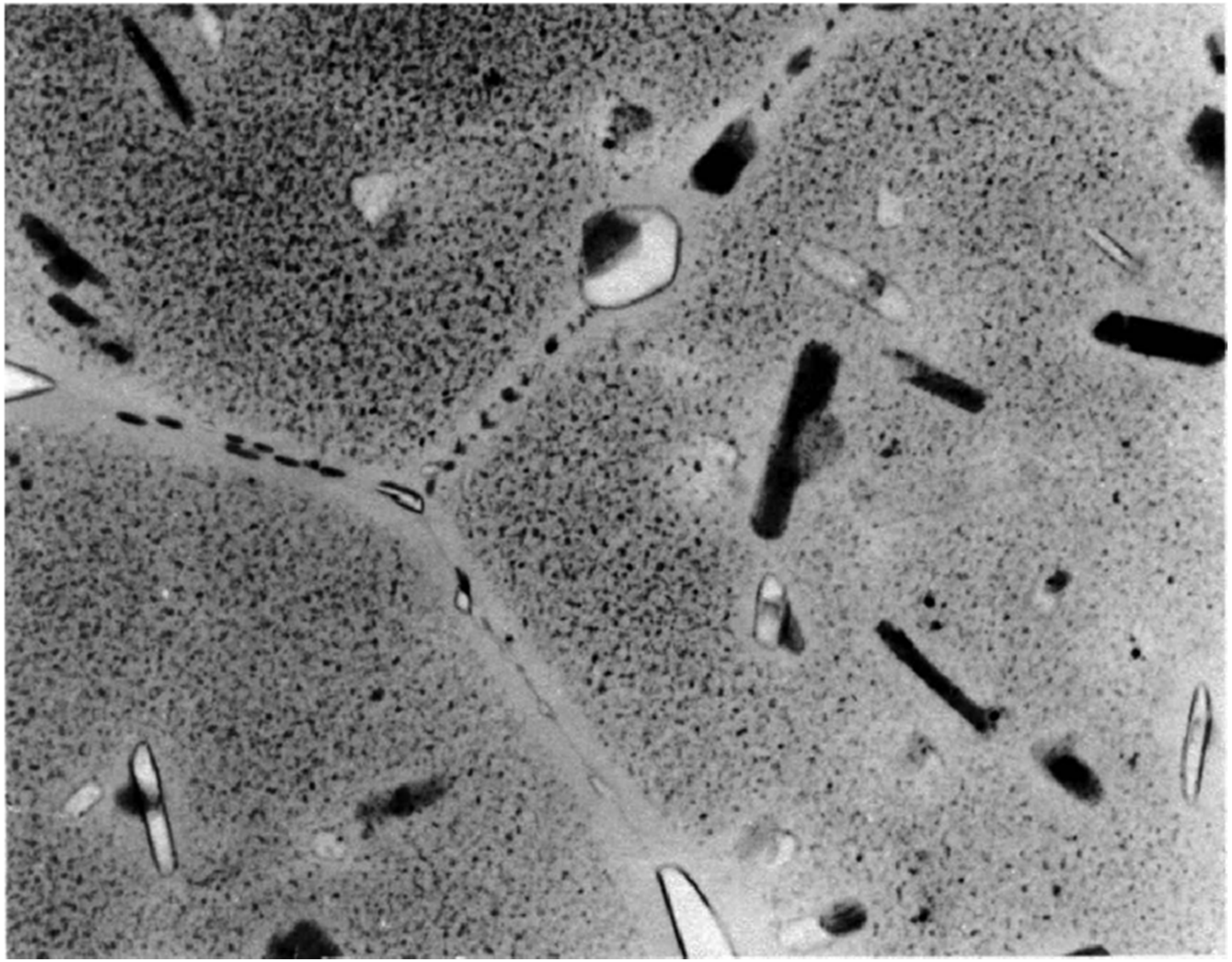

Fig. 5.36 PFZs around grain boundaries in a high-strength commercial Al-Zn-Mg-Cu alloy. Precipitates on grain boundaries have extracted solute from surrounding matrix. (x 59,200)

Q4: Age Hardening

5.5.4. Age Hardening

Transition phase precipitation → great improvement in the mechanical properties

Coherent precipitates→highly strained matrix→the main resistance to the Ⓓ movement: solid solution hardening

Hardness vs. Time by Ageing

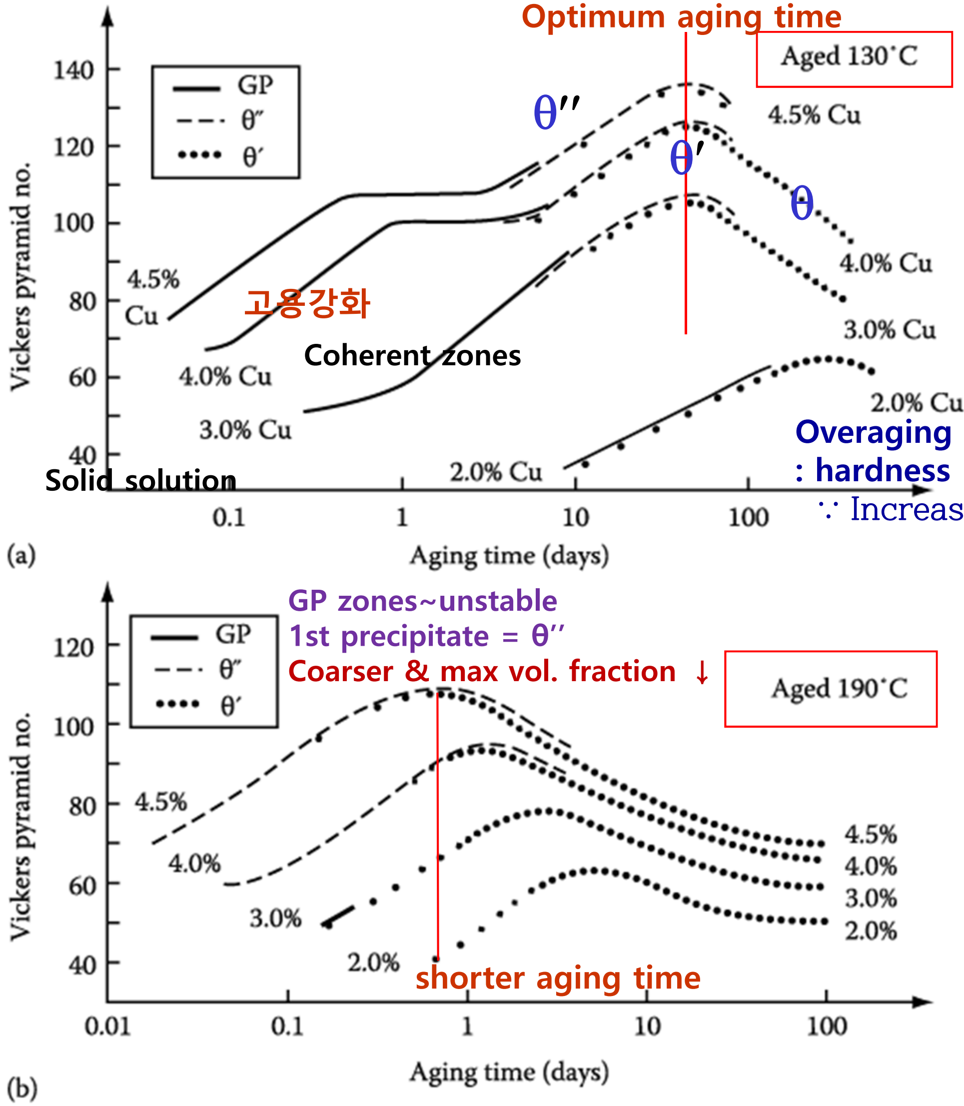

Overaging

: hardness begins to decrease

∵ Increases the distance btw precipitates making Ⓓ bowing easier

Fig. 5. 37 Hardness vs. time for various Al-Cu alloys at (a) 130 ℃ (b) 190 ℃

Maximum hardness~ largest fraction of θ″
(coherent precipitates)

Ageing at 130°C produces higher maximum hardness than ageing at 190°C.

At 130°C, however, it takes too a long time (several tens of days).

How can you get the high hardness for the relatively short ageing time (up to 24h)?

Double ageing treatment

first below the GP zone solvus
→ fine dispersion of GP zones
then ageing at higher T.

: Engineering alloys are not heat treated for max. strength alone. **→ to optimize other properties**
best heat treatment in practice